Systemic Economic Importance and Robustness to Trade Shocks under Uncertainty

Anna Yeganeh Hillingdon
School of Finance and Management, SOAS University of London

Pasquale Scaramozzino
Dipartimento di Economia e Finanza, Università di Roma Tor Vergata
and School of Finance and Management, SOAS University of London

May 2026

Systemic Economic Importance and Robustness to Trade Shocks under Uncertainty

Abstract

This paper is motivated by shifts in U.S. trade policy that have increased uncertainty for trading partners and created incentives to diversify trade away from the United States as a dominant hub in the global trade network. We derive centrality-based indicators from observed bilateral trade flows to measure systemic influence and evaluate their stability under stochastic trade disturbances. We introduce the Stability-Influence Ratio (SIR) and Mean Absolute Influence Change (MAIC) to evaluate robustness, sensitivity, and the scale of influence responses under uncertainty. We simulate exogenous reductions in trade with a dominant hub and reallocate displaced flows across alternative partners to analyse how aggregate connectivity and countries' relative positions adjust endogenously to network structure. The results reveal three main findings. First, trade shocks generate non-linear responses at both the aggregate and country level. Second, reductions in U.S.-linked trade reduce aggregate connectivity because hub contraction losses dominate redistribution gains at low shock levels. Only beyond an estimated turning point do redirected flows strengthen secondary hubs and generate partial recovery in aggregate centrality. Third, highly central economies remain influential but exhibit greater volatility, while economies with concentrated trade structures experience larger declines in systemic importance. These findings demonstrate that trade policy shocks reduce aggregate connectivity before redistribution effects begin to dominate, and that threshold effects shape systemic outcomes in ways that linear or purely bilateral approaches cannot capture.

1.Introduction

Global trade networks are not static. When a major hub alters its trade policies, trade flows seek new routes and patterns of influence adjust across the network. Recent changes in major economies' trade policies illustrate this dynamic, as countries may reallocate trade toward alternative partners, including highly connected European economies or large Southern states. Systemic influence in trade networks constitutes a structural dimension of economic power, it shapes both vulnerability and leverage in contemporary geopolitical competition.

How do systemic measures of influence in the global trade network respond when different sets of countries absorb displaced trade flows? This paper examines how trade shocks propagate through international trade linkages and reshape systemic economic importance across countries. Evidence from recent sanctions, such as those on Russia, shows that trade rarely disappears. Instead, it diverts through highly connected hubs toward neighbouring or neutral third countries, a shift that triggers effects well beyond directly targeted relationships (Gavoille 2025; Bove et al. 2023; Tse et al. 2024; Yassa and Yılmaz 2025). Comparable dynamics appear in U.S.–China trade tensions (2018 to present), sanctions on Russia (2022 to present), and the 2026 U.S.–Israel conflict with Iran. In the latter instance, disruptions around the Strait of Hormuz demonstrate how trade restrictions and geopolitical shocks reroute flows through third countries and generate wider network effects beyond the directly affected economies.

The global trade system exhibits a persistent hierarchical structure in which a small number of countries play a disproportionate role in connecting regions and value chains (Serrano and Boguñá 2003; Garlaschelli and Loffredo 2005; Fagiolo et al. 2009). Production and supply-chain linkages transmit shocks across firms and sectors, allowing disturbances to generate aggregate effects that exceed their initial magnitude (Acemoglu et al. 2012; Barrot and Sauvagnat 2016; Carvalho et al. 2021). The stability of countries' relative systemic positions further depends on how centrality measures respond to uncertainty and trade disturbances, which is shaped by the structure of trade linkages and metric specification (Borgatti et al. 2006; Boldi and Vigna 2014; Segarra and Ribeiro 2016).

While these studies establish the importance of network structure, important limitations remain. Much of the trade-network literature treats observed trade flows as fixed outcomes, limiting its ability to capture uncertainty or dynamic redistribution (e.g., Fagiolo et al., 2009; De Benedictis and Tajoli, 2011). Models of trade diversion typically analyse adjustment through bilateral or linear responses, while robustness analyses are often conducted on stylised or simulated networks rather than observed trade systems (e.g., Segarra and Ribeiro, 2016). As a result, existing approaches do not jointly account for uncertainty, shock propagation, and network structure when evaluating systemic economic importance.

Related evidence also highlights the role of uncertainty. Geopolitical risk reduces national trade openness (Yan and Piao 2025), while trade policy uncertainty generates non-linear firm responses (Liu and Zhang 2025). Countries' positions in trade agreements influence economic development outcomes (Fan et al. 2025), and policy-driven trade initiatives alter countries' positions within global trade networks (Lu et al. 2024). However, these studies focus primarily on country- or firm-level outcomes, with more limited attention to how shocks reshape system-level influence through the trade network itself.

To address this gap, we develop a network-based analytical framework that combines stochastic uncertainty with counterfactual trade redistribution in empirically observed international trade networks (Figure 1). Influence is measured using Katz–Bonacich centrality, and robustness is assessed through random trade disturbances applied to the bilateral trade matrix. The analysis introduces a Stability–Influence Ratio linking baseline influence to sensitivity under uncertainty. The model simulates progressive reductions in trade with a dominant hub, redistributing displaced flows across alternative partners and allowing influence to adjust endogenously to network structure.

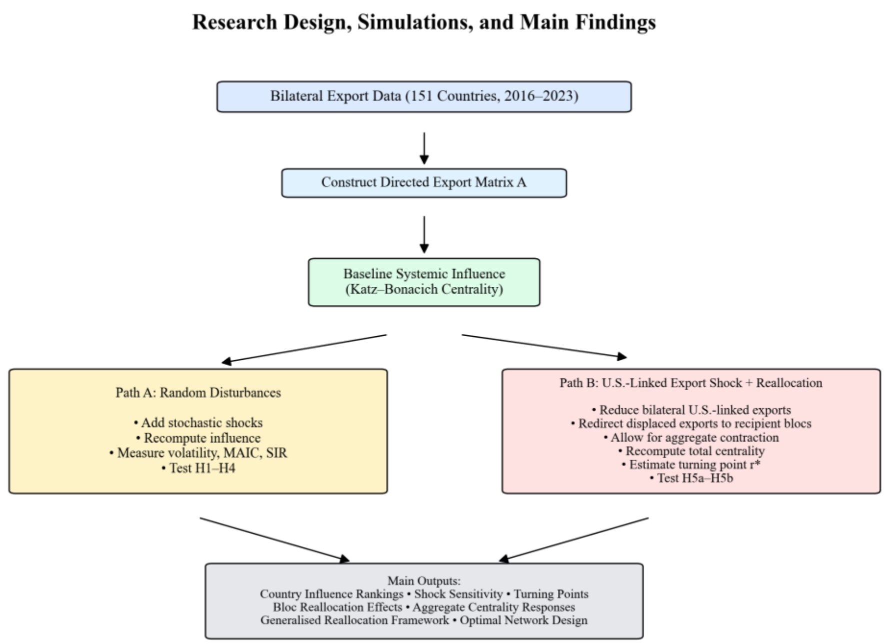

Figure 1. Baseline influence is measured from directed export networks using Katz–Bonacich centrality. Robustness is evaluated under random disturbances using MAIC and SIR. Structured reductions in U.S.-linked exports examine redistribution effects and threshold responses. A uniform global contraction scenario provides a benchmark without reallocation.

This framework makes three contributions. First, it extends the centrality–robustness literature by applying disturbance-based robustness analysis to empirical trade networks. Second, it integrates uncertainty and redistribution within a unified framework, so that systemic influence becomes endogenous to shocks and network topology rather than being treated as fixed. Third, it identifies threshold effects and non-monotonic responses in global connectivity, providing a structural explanation for non-linear outcomes documented in empirical studies of uncertainty. Specifically, the Stability–Influence Ratio (SIR) measures a country's systemic influence relative to the volatility of that influence under simulated trade disturbances, distinguishing robust centrality from fragile prominence. The paper shifts attention from bilateral trade effects to system-level influence reallocation and provides a tractable framework for evaluating structural vulnerability in global trade networks. This framework offers a basis for assessing the systemic consequences of trade policy interventions and geopolitical disruptions in an increasingly interconnected global economy.

2. Literature review and Hypotheses development

The aggregate impact of trade-policy shocks depends on how production and trade linkages transmit disturbances across countries. Theoretical contributions show that network structure can amplify idiosyncratic disturbances and transform them into aggregate fluctuations (Acemoglu et al. 2012). Subsequent work identifies conditions under which interconnectedness produces systemic vulnerability and non-linear aggregate responses (Acemoglu et al. 2015; Elliott et al. 2014). Empirical evidence using firm- and establishment-level data demonstrates that indirect exposure through production linkages can be as important as direct exposure in explaining output, employment, and profitability losses following disruptions (Barrot and Sauvagnat 2016; Boehm et al. 2019; Carvalho et al. 2021). Cross-country input–output analyses similarly show that shocks can diffuse through production networks and generate cascade effects whose magnitude depends on intersectoral structure (Alatriste Contreras and Fagiolo 2014).

Cross-border evidence confirms these transmission mechanisms. Chen (2025), for example, finds that financial shocks originating in the United States propagate strongly to Mexico through production connections. Evidence from sanctions and geopolitical disruptions similarly documents substantial trade diversion toward neutral third countries, weakening the intended effects of restrictions (Scheckenhofer et al. 2025). Dynamic disequilibrium input-output models incorporate inventories, idle capacity, and adjustment frictions to capture short-run disequilibrium dynamics, though these approaches are computationally intensive and difficult to link to measures of systemic importance (Pichler et al. 2022).

International trade exhibits strong heterogeneity in connectivity, with a core group of countries occupying highly central positions in the global trade network (De Benedictis and Tajoli 2011). Early empirical work shows that the world trade system displays a dense and hierarchical structure, with hub economies linking regions and value chains (Serrano and Boguñá 2003; Garlaschelli and Loffredo 2005). Weighted representations of trade flows reveal persistent asymmetries in intensity and direction (Fagiolo et al. 2009), and subsequent analyses document stable core–periphery configurations in which a limited set of countries sustain global integration (Squartini et al. 2011; De Benedictis and Tajoli 2011). More recent research examines resilience and higher-order interdependencies, showing that relatively small changes in trade flows can alter countries' systemic importance (Ren et al. 2024; Ignatenko et al. 2025). Evidence from recent global disruptions further indicates that while bilateral flows may adjust rapidly, the broader structure of the trade network remains persistent (Cerina et al. 2015). Countries' positions within this structure are associated with economic outcomes and may evolve following major policy interventions (Fan et al. 2025; Lu et al. 2024).

A related methodological literature examines how measures of systemic importance respond to data uncertainty and structural changes in observed trade linkages. Empirical centrality rankings can be sensitive to missing or mismeasured trade relationships, and their stability depends on both the structure of trade linkages and the specification of the centrality metric (Borgatti et al. 2006; Boldi and Vigna 2014). In weighted networks, commonly used measures such as degree, closeness, and eigenvector centrality tend to exhibit relative stability, whereas betweenness centrality can display discontinuous shifts when small changes in bilateral trade flows reroute shortest paths (Brandes and Fleischer 2005; Segarra and Ribeiro 2016). Subsequent research shows that sensitivity reflects not only the properties of the metric itself but also the spectral and structural characteristics of the underlying trade network (Martin et al. 2014).

Across these literatures, researchers typically model shock propagation as linear or piecewise and often impose trade reallocation exogenously, abstracting from network structure as a source of amplification. Although non-linear responses to trade policy shocks have been documented at the firm level (Liu and Zhang 2025), their implications for system-level influence and cross-country transmission within global trade networks remain less understood. This study examines settings with uncertain trade flows and analyses how network linkages shape changes in systemic economic importance.

Countries differ in their initial positions within the global trade system, and prior research shows that systemic importance depends on network structure and indirect linkages (Acemoglu et al. 2012; Elliott et al. 2014). Economies occupying more central positions are connected to a larger set of partners and transmission channels, increasing their exposure to disturbances transmitted through the network (Barrot and Sauvagnat 2016; Carvalho et al. 2021). Because systemically important countries receive and transmit shocks through multiple indirect channels, fluctuations in trade flows may induce larger changes in their measured systemic importance (De Benedictis and Tajoli 2011; Fagiolo et al. 2009). Based on these theoretical considerations, we formulate the following hypothesis:

H_1. Higher baseline systemic importance is associated with greater volatility in influence following shocks.

Trade transmission operates through both direct bilateral relationships and indirect linkages across the system (Acemoglu et al. 2012). When indirect connections become more influential, shocks can propagate through longer chains of relationships rather than remaining localised, increasing their aggregate impact (Chaney 2014). This implies that stronger indirect transmission channels can amplify the response of systemic influence to shocks, particularly when propagation effects are non-linear (Baqaee and Farhi 2019). This mechanism predicts:

H_2. Stronger indirect trade linkages amplify countries' systemic influence responses to shocks.

Countries differ substantially in the concentration of their trade relationships. Economies whose trade is concentrated among a small number of partners are more exposed to shocks affecting those partners, whereas more diversified trade structures provide partial insulation against disturbances (Acemoglu et al. 2012). This implies that higher trade concentration increases the sensitivity of systemic influence to shocks. This argument suggests:

H_3. Countries with more concentrated trade structures experience greater volatility in systemic influence under trade disturbances.

Responses to shocks are not necessarily linear (Baqaee and Farhi 2019). Prior research on interconnected systems shows that structural thresholds and non-linear dynamics can emerge when disturbances propagate through networks (Acemoglu et al. 2015; Elliott et al. 2014). Countries with initially lower systemic importance may therefore experience disproportionate changes if shocks alter the structure of connections on which their influence depends (Acemoglu et al. 2012). This suggests that non-linear effects may disproportionately affect countries with lower baseline systemic importance. These insights imply:

H_4. Non-linear propagation effects disproportionately affect countries with lower baseline systemic importance.

At the aggregate level, shock responses may also exhibit threshold behaviour.

H_5a. Aggregate systemic centrality responds non-linearly to reductions in U.S.-linked trade. It declines under low and moderate shocks, reaches a minimum at a critical level of disruption, and then partly recovers when shocks become larger.

This U-shaped aggregate respons**e** implies a threshold at which the marginal effect of additional shocks changes sign. Before this point, losses from weaker trade linkages with a dominant hub reduce total centrality. Beyond it, redistributed trade flows strengthen connectivity and partly offset these losses. The location of this turning point also depends on the structure of recipient blocs, including their internal trade density, scale, and capacity to transmit gains through indirect network paths. Accordingly, the effect of shocks differs across regimes separated by a critical threshold. This implies:

H_5b. The relationship between trade shocks and aggregate systemic centrality exhibits a threshold effect, with negative marginal effects below the turning point and positive marginal effects above it.

3. Methodology

3.1 Data source and sample

This study uses annual bilateral export data for 151 countries over the period 2016–2023, the latest year available at the time of writing, from the World Integrated Trade Solution (WITS) database.

The sample includes all countries for which the relevant trade data are available. For each year, we construct a bilateral trade matrix $\boldsymbol{A} = [a_{ij}]$, where each element a_{ij} denotes exports from country i to country j, measured in thousands of U.S. dollars. Diagonal elements are set to zero. This formulation preserves the directional nature of trade.

3.2. Construction of bilateral trade matrix

Let $A \in \mathbb{R}^{n\times n}$denote a directed bilateral trade matrix, where each element a_{ij} represents an export flow from country i to country j, and $a_{ii} = 0$ indicates the absence of domestic self-export. This specification preserves asymmetric trade dependencies between exporters and importers that would be lost under a symmetric representation.

$$\boldsymbol{A} = \begin{pmatrix} 0 & a_{12} & \cdots & a_{1n} \\ a_{21} & 0 & \cdots & a_{2n} \\ \vdots & \vdots & \ddots & \vdots \\ a_{n1} & a_{n2} & \cdots & 0 \end{pmatrix}, a_{ii} = 0. \tag{1}$$

The empirical analysis focuses on export-based networks, which capture outward transmission of trade influence. Import-based extensions are conceptually analogous but omitted for parsimony.

3.3 Measurement of systemic influence

We quantify countries' systemic importance using Katz–Bonacich centrality (Ballester et al. 2006), which captures both direct and indirect trade linkages. The influence vector is defined as

$$v = (I - \phi\boldsymbol{A})^{-1}\mathbf{1}. \tag{2}$$

where $v \in \mathbb{R}^n$ is the vector of country influence scores, $I$is the identity matrix, $\mathbf{1}$ is a vector of ones, and $\phi \in \mathbb{R}_+$ is the propagation parameter that determines the strength of indirect trade transmission. Equation (2) defines systemic influence as the sum of direct and indirect trade connections. A country is influential not only because it trades heavily itself, but also because it is connected to other influential economies. Influence therefore reflects embeddedness in the wider trade network rather than bilateral trade volume alone.

Economically, ϕ determines the extent to which systemic influence depends on higher-order network connections beyond immediate bilateral trade links. Lower values place greater weight on direct relationships, so shocks remain more localised. Higher values increase the importance of indirect paths, so disturbances that affect central economies spread more widely through the network.

To ensure convergence, ϕ must lie in the interval $(0, 1/\lambda_{\max})$, where $\lambda_{\max}$denotes the spectral radius of $\boldsymbol{A}$ (Debreu and Herstein, 1953). In the empirical implementation, the benchmark specification uses $\phi = 0.9/\lambda_{\max}$, which represents a high but admissible transmission regime. Where reported, comparisons with $\phi = 0.5/\lambda_{\max}$ illustrate how weaker network amplification affects the results.

3.4 Simulation design and robustness analysis

We assess the robustness of systemic influence measures by introducing random trade disturbances to the bilateral trade matrix. In this context, robustness refers to the extent to which countries' influence scores, rankings, and broader network patterns remain stable when observed trade flows are subject to uncertainty. These disturbances do not represent a specific policy intervention or economic event. Instead, they provide a neutral benchmark for evaluating the sensitivity of the results to noise in observed trade data. The disturbances capture measurement error, reporting uncertainty, and small unobserved reallocations of trade. The procedure therefore remains agnostic regarding the source or intent of the shocks.

To examine how uncertainty affects countries' systemic influence, we apply disturbance intensities ranging from 10 percent to 90 percent to matrix $\boldsymbol{A}$ and recompute the influence vector v. Let μ denote the mean of positive bilateral trade volumes:

$$\mu = \frac{1}{|S|} \sum_{(i,j) \in S^+} a_{ij} \, , S^+ = \{ (i,j) \mid i \neq j, \, a_{ij} > 0 \}. \tag{3}$$

This provides the benchmark scale used to calibrate shocks relative to typical bilateral trade intensity. Because each matrix entry represents a directed trade flow, we include all non-zero entries and do not restrict to $i < j$. We define a disturbance-to-signal ratio that scales the standard deviation of random trade shocks relative to the average trade flow. For example, at a ratio of 20 percent, the standard deviation is defined as

$$\sigma = NSR \times \mu. \tag{4}$$

This scaling ensures that disturbances are proportional to the typical size of bilateral trade flows, allowing a transparent interpretation of shock intensity as a fraction of average trade. Higher NSR values therefore represent more severe uncertainty environments.

A matrix of random trade shocks $N \in \mathbb{R}^{n \times n}$is then generated. We draw each off-diagonal element independently from a normal distribution with mean zero and variance σ^2, and set the diagonal equal to zero.

$$\boldsymbol{N} = \begin{bmatrix} 0 & n_{12} & \cdots & n_{1n} \\ n_{21} & 0 & \cdots & n_{2n} \\ \vdots & \vdots & \ddots & \vdots \\ n_{n1} & n_{n2} & \dots & 0 \end{bmatrix},\ n_{ij} \sim \mathcal{N}(0, \sigma^2),\ \ i \neq j. \tag{5}$$

This construction does not impose symmetry and allows shocks to affect trade flows in each direction independently. Disturbances are therefore allowed to differ by direction, reflecting asymmetric trade shocks across trading partners.

The disturbed adjusted trade matrix is defined as:

$$\boldsymbol{A}^{adj} = \boldsymbol{A} + \boldsymbol{N}:$$

$$\boldsymbol{A}^{adj} = \begin{bmatrix} 0 & a_{12} + n_{12} & \cdots & a_{1n} + n_{1n} \\ a_{21} + n_{21} & 0 & \cdots & a_{2n} + n_{2n} \\ \vdots & \vdots & \ddots & \vdots \\ a_{n1} + n_{n1} & a_{n2} + n_{n2} & \dots & 0 \end{bmatrix}, \tag{6}$$

This is the post-shock trade network used to recompute influence. To preserve economically meaningful trade values, any negative entries resulting from the addition of trade disturbances are set equal to zero:

$$\boldsymbol{A}_{ij}^{adj} = \max\{0, \boldsymbol{A}_{ij}^{adj}\}$$

The corresponding influence vector under the adjusted trade structure is

$$\boldsymbol{v}^{\text{adj}} = \begin{bmatrix} v_1^{adj} \\ v_2^{adj} \\ \vdots \\ v_n^{adj} \end{bmatrix} = (\boldsymbol{I} - \phi \boldsymbol{A}^{adj})^{-1}\mathbf{1}. \tag{7}$$

Equation (7) shows how shocks to bilateral trade flows alter systemic influence once the network readjusts. Even localised disruptions can affect multiple countries because influence depends on indirect pathways as well as direct trade links. The resulting change in influence therefore reflects both the magnitude of the disturbance and the structure of the network through which it is transmitted.

In addition to the baseline network assumptions, we require that the scale of the disturbance matrix remain small relative to overall trade intensity. Specifically, we assume that

$$\frac{\|N\|_F}{\|A\|_F} \ll 1, \tag{8}$$

where $\|\cdot\|_F$ denotes the Frobenius norm. This condition ensures that simulated trade adjustments remain modest relative to aggregate trade volumes. It also implies that the spectral radius of **A**+**N** remains close to that of **A**, thereby preserving the stability region for ϕ. Moreover, it supports the validity of the first-order approximation in Proposition 1.

In the simulations, low values of the disturbance-to-signal ratio correspond to small trade-adjustment environments, while higher values function as stress scenarios that explore the limits of the linear approximation. In the empirical implementation, the expected Frobenius norm of the disturbance matrix is approximately two percent of $\| \boldsymbol{A} \|_F$ at a ten percent disturbance ratio and rises to approximately sixteen percent at a ninety percent ratio.

We define

$$\boldsymbol{G} = (\boldsymbol{I} - \phi \boldsymbol{A})^{-1}, \text{ so that } \boldsymbol{v} = \boldsymbol{G}\mathbf{1}. \tag{9}$$

Equation (9) shows that the influence matrix G governs how trade disturbances affect systemic influence and determines how adjustments in bilateral trade flows transmit through the global trade network. The following propositions provide the formal network-theoretic foundations underlying Hypotheses H1–H4.

Proposition 1 (Influence of Volatility).

Let

$$v^{adj} = (I - \phi(\boldsymbol{A} + \boldsymbol{N}))^{-1}\mathbf{1}$$

and define

$\Delta v = v^{adj} - v$, where $v = (I - \phi\boldsymbol{A})^{-1}\mathbf{1}$.

Under the assumptions above and to first-order in the trade disturbances matrix $\boldsymbol{N}$, the change in influence satisfies the approximation

$$\Delta v \approx \phi\boldsymbol{G}\boldsymbol{N}v. \tag{10}$$

Equation (10) demonstrates that the effect of a shock depends on three factors: the scale of the disturbance, the network's transmission structure, and countries' initial influence levels. Shocks are therefore amplified when they hit highly connected systems or already influential economies. Moreover, the adjustment satisfies the norm bound

$$\| \Delta v \| \lesssim \phi \| \boldsymbol{G} \| \cdot \| \boldsymbol{N} \| \cdot \| v \|. \tag{11}$$

Equation (11) implies that larger shocks, stronger propagation, and higher baseline centrality increase the magnitude of influence changes. Holding $\| \boldsymbol{G} \|$ and $\| \boldsymbol{N} \|$ fixed, the magnitude of Δv grows proportionally with $\| v \|$. Countries with higher baseline influence therefore experience larger absolute changes under identical trade disturbances. The propagation parameter ϕ scales this sensitivity linearly: higher values of ϕ amplify the transmission of trade shocks through indirect linkages.

Proof. See Appendix A

Proposition 2 (Concentration and Hub Dependence)

Let the first-order change in influence satisfy equation 10. The component-wise effect for country i is:

$$\Delta \boldsymbol{v}_i \approx \phi \sum_{j=1}^{n} \sum_{k=1}^{n} \boldsymbol{G}_{ij} \boldsymbol{N}_{jk} \boldsymbol{v}_k . \quad (12)$$

[1]

If country i's trade is concentrated among a small number of partners, especially partners with high systemic influence, disturbances affecting those relationships generate larger changes in v_i. Concentration around major hub economies can therefore increase both network relevance and exposure to shocks. More diversified trade structures tend to reduce partner-specific vulnerability, other things equal.

Remark. Proposition 2 implies that trade dependence on influential hubs creates a trade-off between access to central markets and resilience to disturbances

Proposition 3 (Higher-order expansion and limitations).

Under the same assumptions as Proposition 1, the inverse matrix with trade disturbances admits the series expansion

$$(I - \phi(\boldsymbol{A} + \boldsymbol{N}))^{-1}\mathbf{1} = v + \phi \boldsymbol{GN} v + \phi^2 \boldsymbol{GNGN} v + \cdots . \quad (13)$$

Equation (13) implies that small shocks may have approximately linear effects, but larger shocks generate feedback loops through repeated network interactions. This provides the theoretical basis for threshold and non-linear responses observed in the simulations.The first-order approximation $\Delta v \approx \phi \boldsymbol{GN} v$ neglects higher-order terms of order $O(\| \boldsymbol{N} \|^2)$. Consequently, the linear sensitivity bound in Proposition 1 holds asymptotically for sufficiently small trade disturbances. For larger disturbance magnitudes, or when ϕ approaches the stability threshold $1/\lambda_{\max}(\boldsymbol{A})$, higher-order non-linear effects become important and the linear approximation may break down. Proposition 1

[1] Here i denotes the focal country, j the origin of the trade adjustment, and k the partner country associated with affected bilateral trade flow. The term G_{ij} captures how trade adjustments originating in country j transmit through the network to affect country i. The element N_{jk} represents a random adjustment in the bilateral trade flow between countries j and k, and v_k is the baseline influence of country k.

should therefore be interpreted as a local sensitivity result. The simulation results explore behaviour across a broader range of noise-to-signal ratios.

Propositions 1 to 3 characterise the theoretical response of influence scores to random trade disturbances. We now translate these theoretical insights into empirical measures computed from simulations. For each country, we quantify the variability of influence across multiple simulated trade adjustment scenarios, thereby operationalising the theoretical sensitivity bounds and motivating the construction of stability metrics.

For each country i, volatility σ_{v_i} is measured as the mean absolute deviation from its baseline influence across all simulated trade disturbance scenarios:

$$\sigma_{v_i} = \frac{1}{K}\sum_{k=1}^{K} | v_i^{noisy,k} - v_i |. \tag{14}$$

Here, K denotes the number of simulations, $v_i^{adj,k}$ is the influence of country i in the k-th simulated trade adjustment, and v_i is the baseline influence score. Appendix B provides a numerical illustration of this calculation for the United States.

To complement this measure, we define the Stability-Influence Ratio (SIR) as

$$SIR_i = \frac{v_i}{\sigma_{v_i}}. \tag{15}$$

Equation (15) measures how much systemic influence a country retains relative to the volatility of that influence under uncertainty. High values indicate robust influence, while low values indicate fragile prominence. The SIR therefore captures the balance between centrality and volatility, distinguishing between robust and fragile forms of systemic importance. Importantly, the SIR is a diagnostic measure of sensitivity and systemic positioning, and does not represent a welfare or policy optimality indicator.

The mean absolute deviation captures volatility relative to baseline influence. We also compute the Mean Absolute Influence Change, which measures the average magnitude of influence changes across simulations irrespective of baseline size. This distinction separates proportional instability from absolute responsiveness and allows us to assess the role of trade concentration, as captured by the Herfindahl-Hirschman Index.

The Mean Absolute Influence Change for country i is defined as

$$MAIC_i = \frac{1}{L}\sum_{l=1}^{L} \mid \Delta v_{il} \mid. \tag{16}$$

Here, Δv_{il} denotes the change in influence for country $i$under the l-th noise realisation. MAIC captures the average magnitude of influence changes across shock scenarios, regardless of whether those changes are positive or negative. It therefore measures responsiveness rather than rank stability.

The random trade disturbance simulations capture sensitivity to diffuse and unsystematic fluctuations in bilateral trade flows. In practice, trade disruptions often arise as targeted and exogenous shocks. In the next section, we therefore examine simulated reductions in trade with major hub economies, including the United States, and analyse how displaced trade flows redistribute across the network and reshape systemic influence beyond random disturbances.

3.5 Redistribution of Lost Export Flows

We redistribute export volume previously destined for the United States across a selected subset of countries $\varepsilon \subset \{1, \dots, n\}$. The mechanism captures a stylised export-diversion response in which countries facing lower access to the U.S. market redirect exports toward alternative destinations. At the same time, weaker trade ties with the United States reduce imports from the U.S., so the shock combines trade reallocation with partial contraction. We do not assume unilateral expansion by a single country. Instead, redirected export flows are reallocated bilaterally among recipient countries to simulate the creation of new export links. Countries with larger internal export activity absorb a greater share of redirected flows, reflecting differences in market depth and absorptive capacity. The rule preserves the volume of redirected exports within the redistribution mechanism and ensures that network topology determines the resulting responses.

For each country $i \in \mathcal{E}$, total bilateral export activity within the group is defined as

$$\tau_i = \sum_{\substack{j \in \mathcal{E} \\ j \neq i}} \boldsymbol{A}_{ij}(r), \forall i \in \mathcal{E}. \tag{17}$$

Normalised redistribution weights are then defined as

$$w_i = \frac{\tau_i}{\sum_{k \in \mathcal{E}} \tau_k}, \tag{18}$$

where w_i denotes the share of redistributed trade absorbed by country i. The redistributed trade volume between any two countries $i, j \in \mathcal{E}$ equals

$$R_{ij} = w_i w_j T_{\text{lost}}. \tag{19}$$

where T_{lost}denotes the reduction in exports previously destined for the United States.

This redistribution rule provides a transparent baseline. Appendix C provides a numerical illustration of its implementation. We also examine alternative rules for reallocating lost export flows. These include equal allocation across recipient countries and allocation weighted toward baseline network centrality. Across these alternatives, the qualitative response of total network centrality to U.S. export shocks remains unchanged. Moderate export reductions initially reduce aggregate centrality, while larger shocks weaken the decline and may generate partial recovery. Differences across alternative allocation schemes affect the magnitude and timing of the response but not its shape. Appendix D defines the alternative redistribution schemes formally.

The final shock-adjusted export network is defined as

$$\widetilde{\boldsymbol{A}}(r) = \boldsymbol{A}(r) + \boldsymbol{R}(r), \tag{20}$$

where $\boldsymbol{A}(r)$captures the reduction in export flows involving the United States and $\boldsymbol{R}(r)$records redirected export flows among countries in $\mathcal{E}$. The export matrix is directed, so we do not impose symmetry on $\widetilde{\boldsymbol{A}}(r)$.

The influence vector under the shock-adjusted network is measured using Katz–Bonacich centrality,

$$v(r) = (I - \phi\widetilde{\boldsymbol{A}}(r))^{-1}\mathbf{1}, \tag{21}$$

where $\phi < 1/\lambda_{\max}(\boldsymbol{A})$ensures invertibility for all values of $r$considered. Equation (21) captures how systemic influence changes after exports are diverted away from the United States and reallocated across alternative partners. Influence is therefore endogenous to how trade is rerouted, and the resulting influence vector is fully determined by the adjusted trade structure.

Remark 4. Decomposition of the marginal effect of trade shocks

Let $\widetilde{\boldsymbol{A}}(r)$denote the adjusted export network following a proportional reduction of size $r \in [0,1)$in exports to the United States, together with lower imports from the United States and redistribution to the set $\mathcal{E}$. Let total network centrality be defined as

$$C(r) = \mathbf{1}^{\top} v(r).$$

Differentiating $C(r)$ with respect to r yields

$$\frac{dC}{dr} = \mathbf{1}^{\top}(I - \phi\widetilde{\boldsymbol{A}}(r))^{-1}\phi\frac{d\widetilde{\boldsymbol{A}}(r)}{dr}v(r),$$

which can be decomposed as

$$\frac{dC}{dr} = \underbrace{\mathbf{1}^{\top}((\boldsymbol{I} - \phi\widetilde{\boldsymbol{A}}(r))^{-1}\phi\frac{d\boldsymbol{A}(r)}{dr}\ \boldsymbol{v}(r)}_{\text{reduction term(negative)}} + \underbrace{\mathbf{1}^{\top}((\boldsymbol{I} - \phi\widetilde{\boldsymbol{A}}(r))^{-1}\phi\frac{d\boldsymbol{R}}{dr}v(r)}_{\text{redistribution term (positive)}} \tag{22}$$

Equation (22) decomposes the marginal effect of a trade shock into two opposing forces: reduced trade with a dominant hub lowers aggregate connectivity, while reallocation toward alternative partners can offset part of that loss. The balance between these forces generates non-monotonic outcomes. The first term captures the direct loss of export flows associated with reduced access to the U.S. market and weaker imports from the United States, and is negative under the model specification. The second term captures the indirect effect of reallocating lost exports toward countries in $\mathcal{E}$, and is positive whenever redistribution expands export flows among those nodes. The marginal effect of an export shock is therefore generally non-monotonic and depends on the relative strength of these two channels.

If the reduction effect dominates at small values of r, total network centrality declines relative to its pre-shock level. As the shock intensifies, redistribution gains can offset part of these losses, causing the marginal effect to turn positive. The mechanism suggests the existence of a threshold shock size r^*at which total network centrality reaches a minimum.

Entry-wise, the redistribution component of the marginal effect can be written as

$$\frac{dC}{dr}\Big|_{redistribution} = \sum_{i\in\varepsilon}\sum_{k=1}^{n}[\left(\boldsymbol{I}-\phi\widetilde{\boldsymbol{A}}(r)\right)^{-1}]_{ki}\frac{d\boldsymbol{R}_{ki}}{dr}\boldsymbol{v}_i(r)^2 \tag{23}$$

Equation (23) implies that redistribution is most effective when diverted trade flows are directed toward countries that are both well connected and able to transmit gains through the wider network. The impact therefore depends on the interaction between network propagation, the allocation of redirected exports, and the baseline influence of recipient countries. Redistribution toward highly influential nodes generates larger immediate effects, whereas redistribution toward weaker nodes becomes more relevant only at larger shock magnitudes.

The empirical analysis that follows operationalises these mechanisms in two steps. First, random export disturbances assess robustness to uncertainty and measure how influence and volatility co-evolve. Second, export reductions and redistribution scenarios examine how shocks to a dominant hub reshape aggregate and country-level influence. These exercises translate the theoretical structure into testable implications about stability, non-linearity, and the redistribution of systemic influence.

4. Empirical Results

This section presents the empirical findings in five parts. We first assess the robustness of systemic influence rankings under random trade disturbances. We then examine the relationship between baseline influence and volatility (H1), evaluate the role of the propagation parameter (H2), analyse the effect of trade concentration (H3), and finally assess the presence of non-linear effects (H4). The results collectively address three related questions: (i) how robust influence rankings are to

[2] The double sum captures the combined effect of the network amplification through all paths in the network (from the inverse matrix) and the current centrality of the recipient node i. Intuitively, each element of $\left(\boldsymbol{I}-\phi\widetilde{\boldsymbol{A}}(r)\right)^{-1}$ measures how a unit of influence at one node propagates through the network, and $\boldsymbol{v}_i$ weights this propagation according to the node's current influence. This decomposition shows why redistribution to nodes with underutilised paths can increase total network centrality more than redistribution to already dominant nodes.

uncertainty in trade data; (ii) how baseline position and trade structure shape volatility; and (iii) whether non-linear amplification emerges as disturbances intensify. To maintain readability, all panel figures in this section are presented for 2021 and 2023. These two years are representative of the full estimation period. Results for the complete sample (2016–2023) are qualitatively unchanged and are available from the authors upon request.

4.1 The robustness of influence rankings under Trade Disturbances

We analyse bilateral trade data on exports from 2016–2023. The analysis is conducted on a sample of 151 countries. Baseline systemic influence is computed using Katz–Bonacich centrality (Eq. 2). In all years China ranks as the most influential country (even without Hong Kong), followed by the United States. We then implement the disturbance procedure described in Section 3.4. The noise-to-signal ratio varies from 10 to 90 percent in increments of 10 percentage points, yielding nine disturbed trade matrices. For each disturbed matrix, we recompute the corresponding influence vector using Equation (7).

To evaluate the stability of influence rankings under trade disturbances, we compute the Spearman rank correlation coefficient between baseline rankings and rankings from disturbed trade matrices. This non-parametric measure captures monotonic agreement in rank order and is well suited to assessing robustness to uncertainty in bilateral trade flows. The results, shown in Figure 2, indicate that Spearman rank correlations remain consistently high across disturbance levels, exceeding 0.88 and remaining statistically significant at the five-percent level. These findings suggest that influence rankings are highly robust to moderate trade disturbances.

Figure 2. Effect of Noise Level on Ranking Stability (2016–2023)

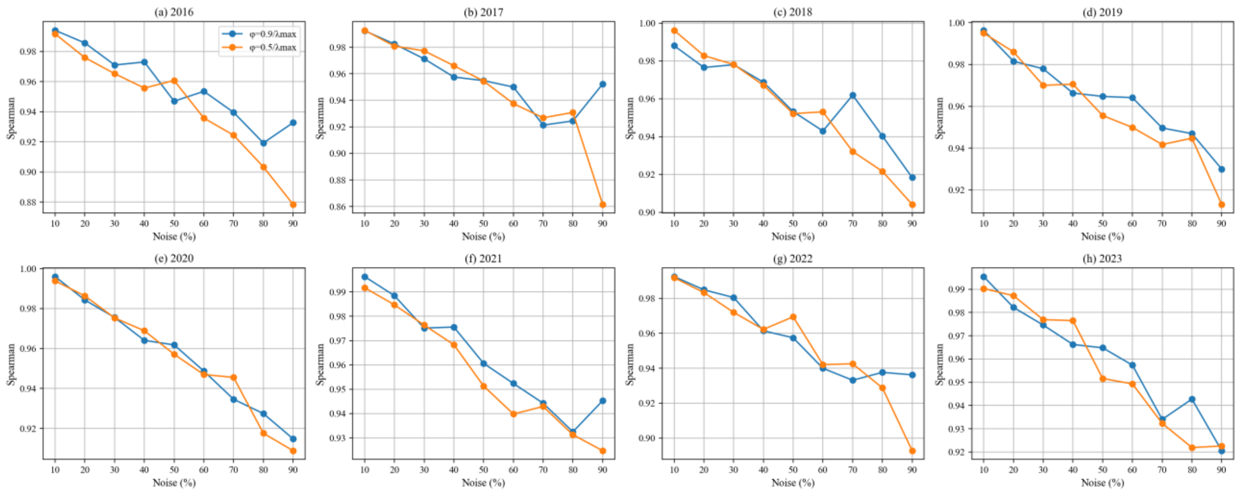

Figure 2 (Spearman rank correlation — referenced in the code but not shared) Spearman rank correlations between baseline Katz–Bonacich centrality rankings and rankings computed under random trade disturbances of increasing intensity (10%–90% noise-to-signal ratio), for 151 countries over 2016–2023, under $\boldsymbol{\phi = 0.9/\lambda_{\max}(A)}$. Values consistently exceed 0.88, indicating that the global hierarchy of systemic trade influence is highly robust to diffuse uncertainty in bilateral export flows. All correlations are statistically significant at the 5% level.

To complement the rank-correlation analysis, we conduct Wilcoxon signed-rank tests comparing baseline influence scores with average influence scores under trade disturbances across different noise levels, for 2016–2023 and for the propagation parameter $\phi = 0.9/\lambda_{\max}(\boldsymbol{A})$. The results indicate statistically significant differences between baseline and disturbed influence scores in all years ($p < 0.001$). This implies that, although rankings remain highly stable, the magnitude of influence changes in response to perturbations in bilateral trade flows. In other words, the global trade network preserves the relative ordering of countries, but not the absolute intensity of their systemic influence.

To further assess robustness, we examine changes in country rankings relative to the baseline over 2016–2023. In the absence of a universal threshold for what constitutes a large rank change, movements of one to two positions in a sample of approximately 150 countries can reasonably be considered minor. For each country, we compute the average absolute rank change across all disturbance levels, capturing the typical deviation from its baseline position under trade uncertainty.

The results reveal a clear pattern across the distribution of influence. Highly central countries exhibit near-zero rank variation, while countries in the middle of the distribution show only small changes. In contrast, countries at the lower end of the influence distribution display substantially larger rank movements. This pattern reflects both structural and mechanical factors. At the core of the network, influence is supported by dense and redundant trade linkages, which stabilise rankings under perturbations. At the periphery, influence scores are closely clustered, so small changes in magnitude can generate frequent reordering. In addition, because disturbance variance is scaled to the average trade flow rather than to country-specific trade intensity, the relative impact of noise is larger for countries with very small trade volumes, amplifying rank variability among peripheral countries.

Despite this heterogeneity, the overall ranking structure remains stable. Changes are concentrated among low-influence countries and do not affect the relative ordering of the most influential economies. This pattern remains unchanged across alternative values of the propagation parameter ϕ, indicating that the concentration of rank variation in the periphery reflects structural features of the trade network rather than the specific choice of propagation intensity. Lower values of ϕ place greater weight on direct bilateral trade links and reduce the contribution of indirect network paths, whereas higher values increase the importance of multi-step transmission through the trade system. The similarity of the results across alternative values therefore indicates that the main conclusions reflect stable structural features of the network rather than a particular calibration of propagation intensity.

4.2. Baseline influence and volatility (H1)

To evaluate Proposition 1, we examine whether countries with higher baseline systemic influence exhibit greater volatility under trade disturbances (H1). We analyse the relationship between baseline influence v_i and volatility $\sigma(v_i)$using correlation analysis and linear regression (Figures 3A–B).

When the propagation parameter is set close to its stability bound ($\phi = 0.9/\lambda_{\max}$), the relationship between baseline influence and volatility is strong, positive, and statistically significant across all years (Figure 3A). Regression slopes are consistently positive, and explanatory power is very high ($R^2 \approx 0.94$–0.95). Pearson correlations are also large (≈ 0.97), confirming a robust positive association between baseline influence and volatility.

By contrast, when the propagation parameter is set to a lower level ($\phi = 0.5/\lambda_{\max}$), the relationship weakens substantially (Figure 3B). While regression slopes remain slightly positive in pooled specifications, explanatory power declines sharply ($\mathrm{R}^2 \approx 0.08$–$0.17$). Pearson correlations are much smaller, and Spearman correlations are negative and statistically significant, indicating a more heterogeneous and non-linear relationship between influence and volatility. The decline in R^2 reflects a weaker common transmission mechanism across countries. When ϕ is low, indirect network spillovers are attenuated, so baseline influence alone explains less of the cross-country variation in volatility. Instead, volatility depends more strongly on structural heterogeneity, including whether countries occupy centre or periphery positions, the composition of trade partners, and the balance between diversification and concentration effects. As a result, a single linear specification provides a substantially poorer fit.

To assess whether this heterogeneity reflects systematic differences across country groups, we conduct Chow tests for structural breaks between centre and periphery countries. Following the centre–periphery tradition, we define centre countries as those occupying the most central positions in the trade network, measured by baseline Katz–Bonacich centrality. The composition of the centre group is highly stable over time. In each year, countries are ranked by their centrality scores, and those in the top decile (above the 90th percentile) are classified as centre countries, while the remaining countries are classified as periphery. The results strongly reject the null of parameter stability ($p \approx 0$ in all cases), indicating that the relationship between influence and volatility differs across these groups.

This is further examined using regressions that include a dummy variable for centre countries and an interaction term with baseline influence (Appendix E). Both the intercept and slope differences are statistically significant. The coefficient on the centre dummy is negative and statistically significant, implying that centre countries exhibit lower volatility than periphery countries at low levels of baseline influence. The interaction term between influence and the centre dummy is positive and significant, suggesting that volatility increases more rapidly with influence for centre countries. This implies a crossover effect: while centre countries are less volatile at low levels of influence, they become more volatile than periphery countries as influence increases.

The effect of baseline influence differs across propagation regimes. When ϕ is high (Figure 3A), both centre and periphery countries show a positive relationship between influence and volatility, with a stronger effect for centre countries. By contrast, when ϕ is low (Figure 3B), the slope for periphery countries turns negative, meaning that higher centrality reduces volatility, while the slope for centre countries stays positive but weaker.

As ϕ increases, influence volatility becomes more pronounced for highly central countries. When ϕ is set close to its stability bound, highly influential countries experience substantially larger fluctuations in influence scores. At lower values of ϕ, influence propagation is more limited, and the relationship between baseline influence and volatility weakens. Under these conditions, diversification effects dominate for periphery countries, while centre countries remain exposed to systemic risk due to their central position in the network.

Structurally, highly influential countries are extensively connected through both direct and indirect trade linkages. Their systemic centrality is associated with a larger spectral radius of the trade matrix, which constrains the admissible range of the propagation parameter ϕ. The parameter must remain strictly below the inverse of the spectral radius to ensure stability. Greater trade density and stronger bilateral linkages increase the spectral radius, thereby limiting the admissible range of ϕ and constraining overall amplification. Nonetheless, highly central economies, such as the United States and China, remain disproportionately sensitive to trade disturbances, as shocks affecting them propagate through multiple direct and indirect linkages.

The results provide strong support for H1 in high-propagation regimes, where higher baseline influence is consistently associated with greater volatility. However, this relationship weakens and becomes conditional when propagation is limited. In particular, the effect of influence depends on countries' positions in the network, with centre countries showing increasing volatility with centrality, while periphery countries may experience stabilising effects at lower levels of propagation.

This pattern reflects differences in trade exposure and network connectivity. Highly central countries maintain extensive direct and indirect trade linkages, so shocks affecting them transmit widely through the network and generate larger fluctuations in their influence. By contrast, less central countries operate with fewer and more localised connections, which limits the transmission of disturbances and can reduce volatility when propagation is low. Thus, the influence–volatility relationship is not uniform, but depends on both network reach and structural position.

Figure 3A. Influence vs Volatility (2021 vs 2023), $\phi = 0.9/\lambda_{\max}(\mathbf{A})$

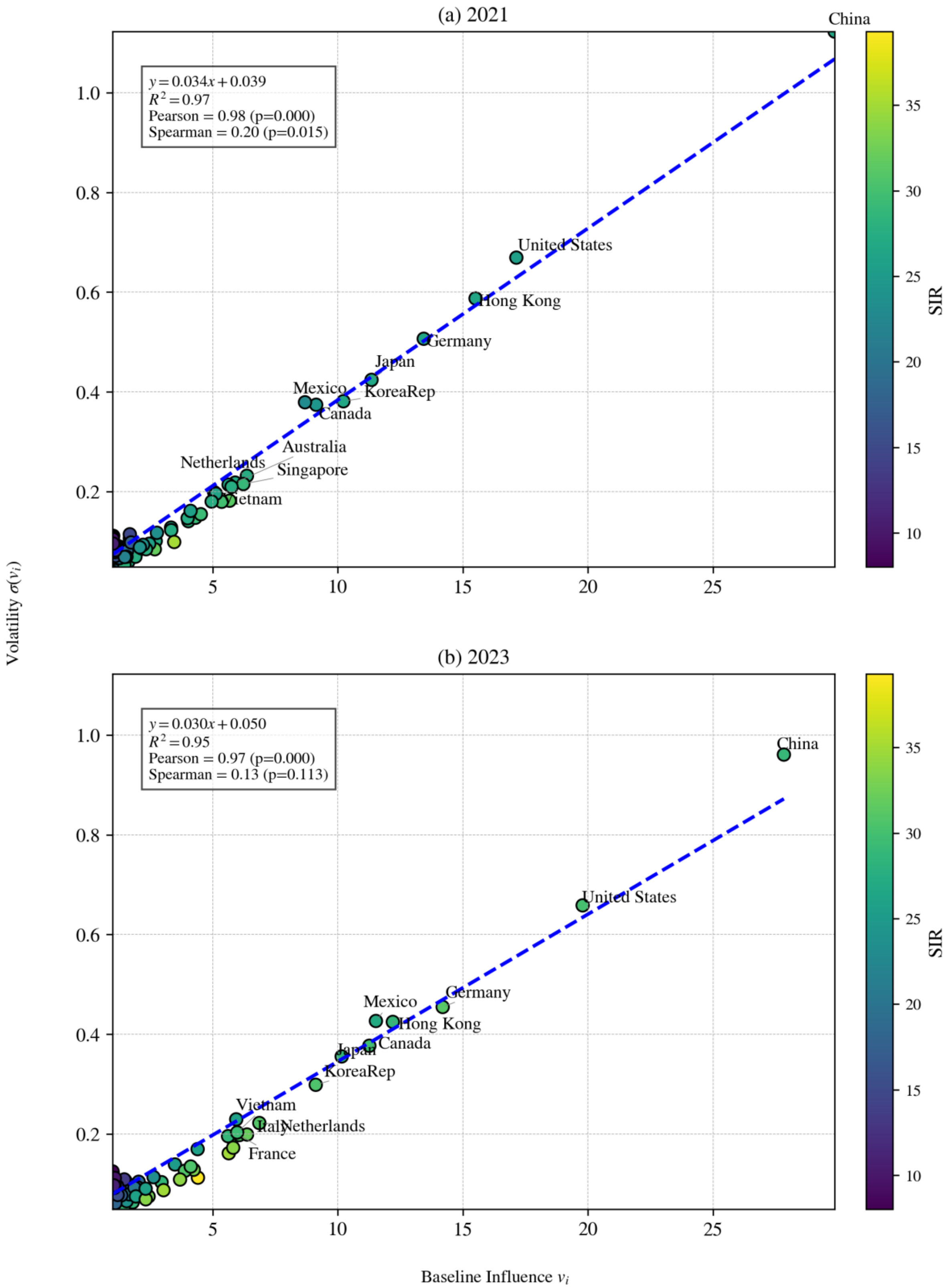

Figure 3B. Influence vs Volatility (2021 vs 2023), $\phi = 0.5/\lambda_{\max}(\mathbf{A})$

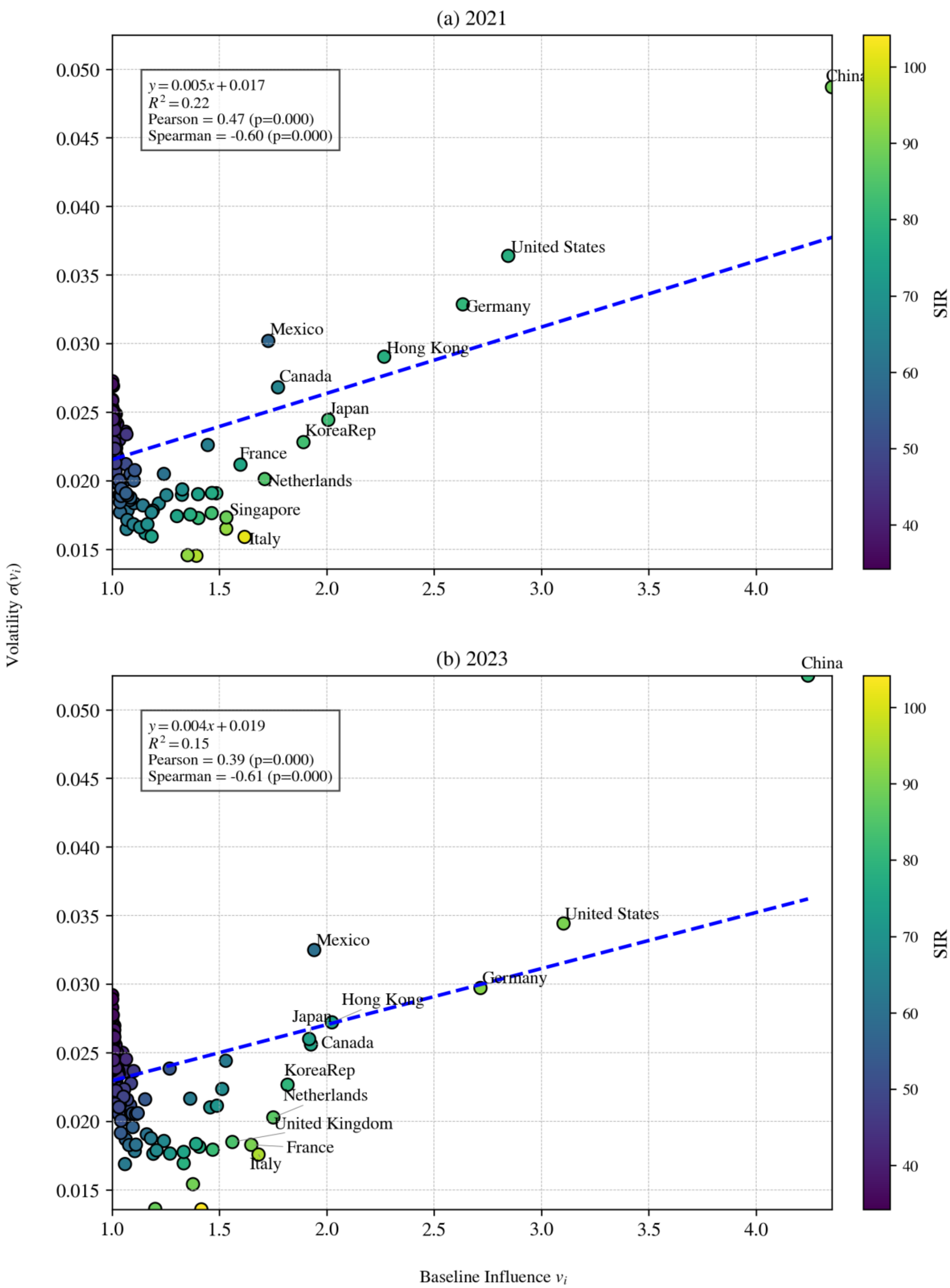

Figures 3A & 3B (influence vs. volatility scatter plots*)* Cross-country relationship between baseline Katz–Bonacich centrality and influence volatility (mean absolute deviation across simulated trade disturbances) for 151 countries, 2016–2023. Figure 3A uses $\phi = 0.9/\lambda_{max}(\mathbf{A})$: the relationship is strongly positive (R^2 = 0.94–0.95; Pearson $r \approx 0.97$), confirming that more systemically important economies exhibit greater sensitivity to shocks. Figure 3B uses $\phi = 0.5/\lambda_{max}(\mathbf{A})$: explanatory power drops sharply (R^2 = 0.08–0.17), reflecting weaker indirect transmission and greater structural heterogeneity between core and peripheral economies.

4.3. Effect of the Propagation Parameter $\boldsymbol{\phi}$ (H2)

This section examines how variation in the propagation parameter ϕ affects the sensitivity of influence outcomes. Holding the magnitude of trade disturbances constant, higher values of ϕ amplify changes in systemic influence.

Empirically, raising ϕ from $0.5/\lambda_{max}$ to $0.9/\lambda_{max}$ produces a systematic amplification of influence responses in each year from 2016 to 2023. Influence vectors computed under the two propagation regimes remain highly correlated throughout this period, with Pearson correlations ranging from 0.9919 to 0.9933 and Spearman correlations ranging from 0.9960 to 0.9969. These values confirm that changes in ϕ do not materially alter the relative ordering of countries. However, the magnitude of influence responses increases under higher values of ϕ.

Paired t-tests yield statistically significant differences in mean influence responses across the two regimes in every year from 2016 to 2023 ($p < 0.001$ in all cases), with moderate and stable effect sizes (Cohen's d ranging from 0.3826 to 0.4059). These results confirm that higher values of ϕ amplify the transmission of trade disturbances through indirect linkages.

4.4 Trade Concentration and Influence Sensitivity (H3)

To examine Proposition 2, we evaluate whether countries with more concentrated trade portfolios experience larger changes in systemic influence under trade disturbances. Trade concentration for each country $i$is measured using the Herfindahl–Hirschman Index:

$$HHI_i = \sum_j s_{ij}^2 \tag{24}$$

where s_{ij} denotes country i's share of total bilateral exports with partner j.

We test H_3 by estimating annual cross-sectional regressions of MAIC (Mean Absolute Influence Change, i.e. how much a country's influence moves when shocks occur) on trade concentration (HHI) and baseline Katz–Bonacich centrality, and by complementing these estimates with non-parametric rank correlations. A higher MAIC indicates greater sensitivity of systemic influence to disturbances and larger swings in influence outcomes.

The bivariate relationship between HHI and MAIC is positive but modest. Spearman's rho and Kendall's tau remain positive across the sample period, indicating that countries with more concentrated export structures tend to experience larger changes in systemic influence. However, simple linear specifications yield limited explanatory power, which suggests that concentration alone does not fully account for cross-country differences in vulnerability. This weak bivariate fit is consistent with the visual evidence: countries can display high influence sensitivity either because exports are concentrated or because they occupy highly central positions in the network. A single concentration measure therefore cannot capture all sources of vulnerability.

Once baseline systemic influence is included, the results become substantially stronger. Across years, both HHI and Katz–Bonacich centrality enter positively, and the explanatory power of the model rises sharply. For example, in 2023 the regression explains 95.8 percent of the cross-country variation in MAIC ($R^2 = 0.958$), while both coefficients are positive and statistically significant. The evidence therefore indicates that vulnerability operates through two distinct but complementary channels: export concentration and systemic centrality. In other words, countries become vulnerable either because they depend heavily on a narrow set of export destinations or because they are so central that disturbances propagate back to them through multiple layers of the network.

The economic interpretation is straightforward. Countries with concentrated export portfolios depend more heavily on a narrow set of destination markets and have fewer opportunities to redirect trade when disruptions occur. Disturbances affecting key partners therefore generate larger changes in their network influence. At the same time, highly central economies are deeply embedded in the global export system, so shocks affecting them propagate through multiple direct and indirect linkages. Their own influence scores become more responsive because they occupy the core of a dense web of interdependence.

These relationships are illustrated in Figures 4A and 4B, which map countries according to export concentration (HHI) and Katz–Bonacich centrality, with bubble size proportional to MAIC. Larger bubbles therefore represent countries whose systemic influence is more sensitive to disturbances. The figures make clear that vulnerability is multidimensional. Large influence responses arise either from high concentration, from high systemic centrality, or from the interaction of both forces. This visual evidence complements the regression results by showing how different structural positions in the network generate distinct forms of exposure.

This framework helps explain cases such as Canada and Mexico. Both economies are strongly integrated with the United States and derive substantial network relevance from access to a dominant hub market. Yet this same structure also creates vulnerability. When a large share of exports is tied to a central partner, disturbances affecting that relationship transmit more strongly into domestic influence outcomes. Integration with an influential hub can therefore increase economic importance while simultaneously raising exposure to shocks.

The United States and China remain distinctive cases. Despite relatively diversified export portfolios, both countries exhibit elevated influence sensitivity. Their vulnerability arises less from bilateral concentration and more from their central role in the wider network. Because shocks affecting these economies reverberate across the global system and feedback through many channels, diversification does not eliminate the risks associated with systemic importance.

Comparing alternative values of the Katz attenuation parameter further sharpens this interpretation. When ϕ is low, influence depends more heavily on direct bilateral export relationships, so concentration of export destinations becomes relatively more important. When $\phi$is high, indirect linkages and network spillovers receive greater weight, shifting vulnerability toward globally central hub economies. The contrast between Figures X and Y therefore distinguishes between concentration-based fragility and connectivity-based fragility in the world export system.

Recent research has also emphasized that international trade dynamics reflect forces operating beyond country-specific bilateral relationships. Beck and Jackson (2024) show that global and regional common factors explain a substantial share of cross-country trade fluctuations. This insight is relevant when interpreting differences across blocs, since more integrated groups may respond differently to external shocks than weaker or less connected ones. International interdependence also extends beyond merchandise exports. Dai et al. (2026) find that cross-border technology inflows can influence domestic structural change and productivity growth. These contributions underline that shocks to major economies may transmit internationally through several connected channels.

An important distinction also emerges between volatility in influence levels and stability in influence rankings. Highly central economies may experience relatively large changes in influence magnitude under trade disturbances, yet their rankings remain stable because their baseline advantage over other countries is substantial. By contrast, as shown in Section 4.1, rank variation is concentrated among lower-influence countries, where scores are more tightly clustered and small changes can generate reordering. The global export network therefore combines a stable hierarchy with variable influence intensity.

Figure 4A. Two Channels of Trade Vulnerability: Concentration and Systemic Influence, 2021 & 2023
Computed with $\phi = 0.9/\lambda_{\max}(\mathbf{A})$ • Bubble size denotes MAIC • Labels identify the top 10 countries by MAIC

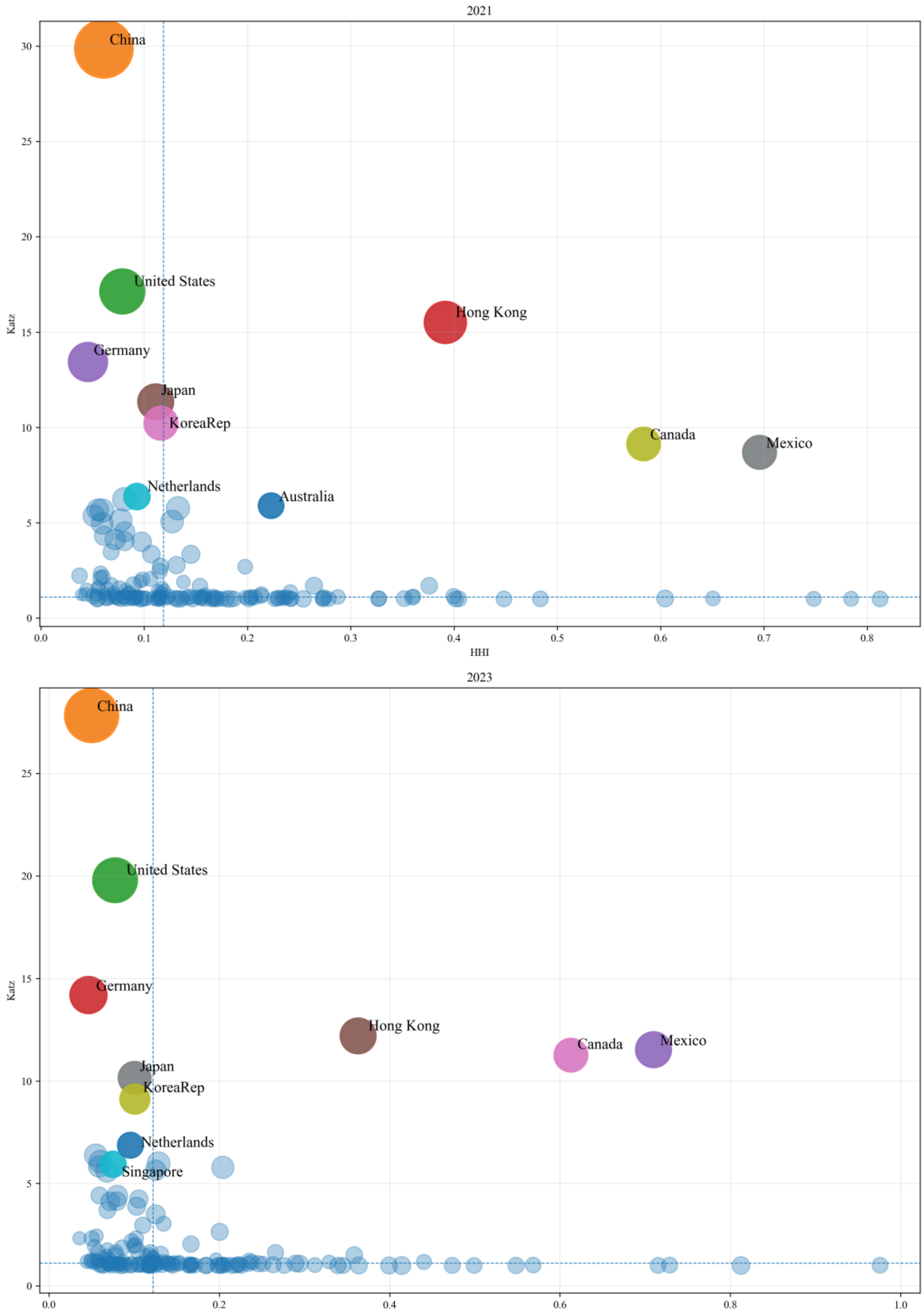

Figure 4B. Two Channels of Trade Vulnerability: Concentration and Systemic Influence, 2021 & 2023
Computed with $\phi = 0.5/\lambda_{\max}(\mathbf{A})$ • Bubble size denotes MAIC • Labels identify the top 10 countries by MAIC

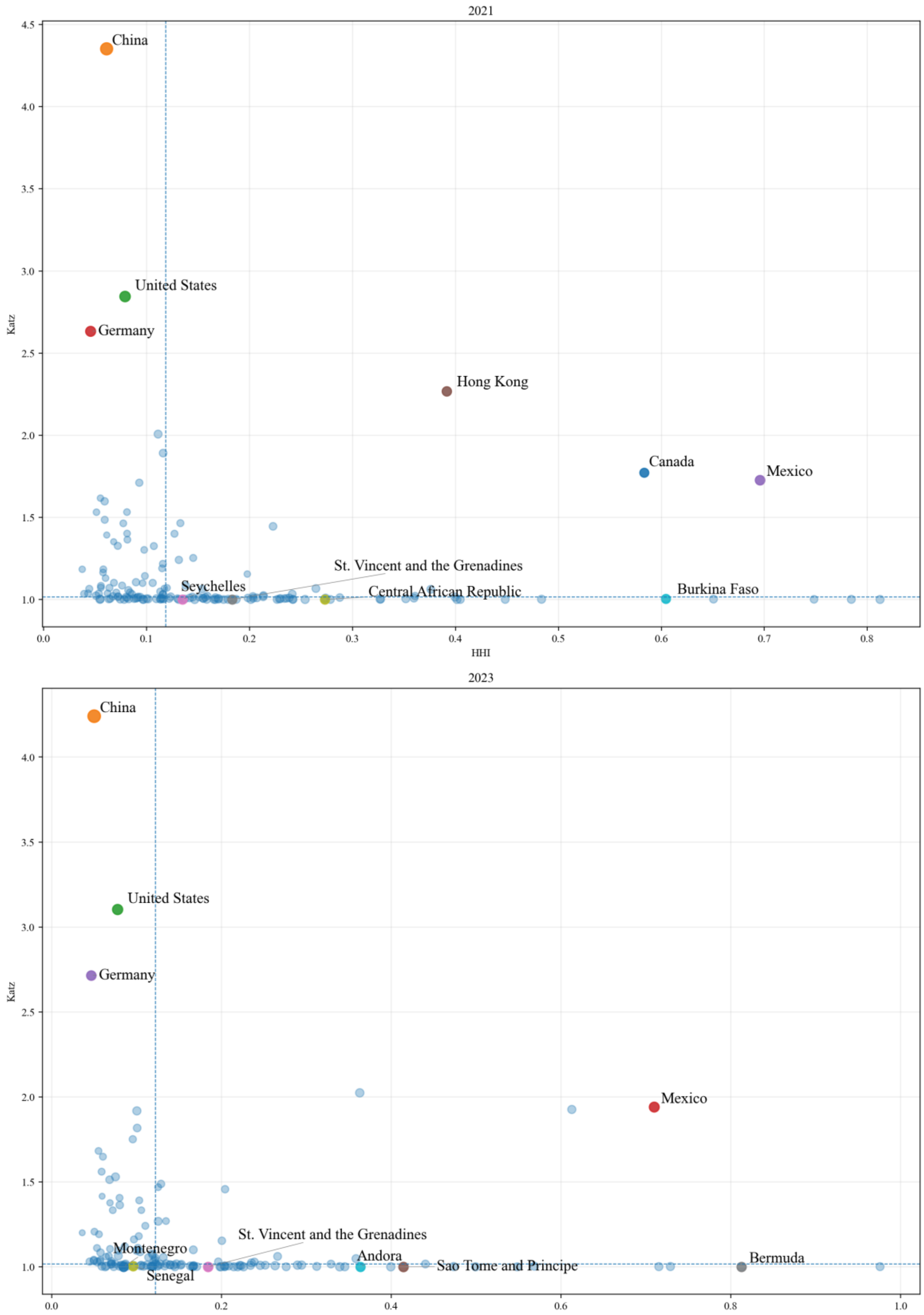

Figures 4A & 4B Bubble charts mapping 151 countries according to two channels of trade vulnerability for 2021 and 2023. The horizontal axis shows export concentration (Herfindahl–Hirschman Index, HHI); the vertical axis shows baseline Katz–Bonacich centrality (Katz); and bubble size is proportional to Mean Absolute Influence Change (MAIC), measuring how much a country's systemic influence responds to random trade disturbances. Dashed lines denote sample medians. Labels identify the ten countries with the largest MAIC values. Figure 4A is computed with $\phi = 0.9/\lambda_{max}(\mathbf{A})$; Figure 4B with $\phi = 0.5/\boldsymbol{\lambda_{max}}(\mathbf{A})$. Countries appearing in the upper-right quadrant combine high systemic centrality with concentrated trade portfolios, making them vulnerable through both channels simultaneously.

4.5: Non-linear effects and relative error (H4)

H_4 predicts that countries with low baseline influence experience larger non-linear deviations and greater rank instability, whereas highly influential economies remain comparatively stable. To evaluate this proposition, we examine how the response of influence changes as trade disturbances intensify and network feedback effects become more pronounced.

The first-order approximation derived in Section 2.3 (Eq. 13) captures the immediate response of influence to small shocks. As disturbances become larger, or as the propagation parameter ϕ approaches its stability threshold $1/\lambda_{\max}(\boldsymbol{A})$, indirect and feedback effects become more important, causing observed outcomes to diverge from the linear benchmark. We measure this divergence using:

$$\text{Relative Error} = 100 \times \frac{\hat{v}^{\,noisy} - (v+\phi GNv)}{v} \tag{25}$$

where $\hat{v}^{\,noisy}$is the simulated influence vector under disturbed trade flows and $(v+\phi GNv)$is the first-order approximation. Larger values indicate that higher-order network effects materially alter the impact of shocks.

The results are characterised by a clear and economically meaningful asymmetry. Highly influential economies consistently record the smallest relative errors across disturbance levels, indicating that their position in the export system is robust even when trade flows are disrupted. By contrast, lower-ranked economies exhibit substantially larger and more volatile deviations, especially at high noise-to-signal ratios. Middle-ranked economies lie between these extremes. Figures 5A and 5B show that this ordering is stable across all years and under both parameter values. Although the absolute magnitude of deviations differs between $\phi = 0.9/\lambda_{\max}(\boldsymbol{A})$ and $\phi = 0.5/\lambda_{\max}(\boldsymbol{A})$, the same pattern persists: countries at the core of the network are more resilient, while peripheral economies are more exposed to disruption.

These differences are statistically significant throughout the sample. For example, in 2016 under $\phi = 0.9/\lambda_{\max}(\mathbf{A})$, a Kruskal–Wallis test rejects equality across groups ($p = 1.94 \times 10^{-6}$), while a Mann–Whitney test confirms a significant gap between the top and bottom groups ($p = 7.43 \times 10^{-7}$). Under the lower propagation regime, the hierarchy remains significant ($\phi = 0.5/\lambda_{\max}(\mathbf{A})$: Kruskal–Wallis $p = 7.86 \times 10^{-5}$; Top vs Bottom $p = 2.95 \times 10^{-5}$). Stronger propagation therefore increases the scale of non-linear effects, but not their unequal distribution across countries. Figures 5A and 5B show that leading economies remain comparatively stable, whereas lower-ranked economies exhibit substantially larger deviations as disturbances intensify.

The economic interpretation is straightforward. Core economies benefit from diversified export markets, broader market access, and multiple indirect channels of transmission. These features absorb local shocks and help preserve their relative standing. Peripheral economies rely on narrower trade relationships and have less scope to offset disruptions through alternative connections. As a result, disturbances generate larger proportional swings in influence and greater ranking volatility. These findings strongly support H_4. The global export network exhibits asymmetric resilience: influence at the core is structurally stable, whereas influence at the periphery is considerably more sensitive to higher-order disturbances.

Figure 5A. Non-linear Effects (Relative Error) under Trade Disturbances, 2021 & 2023

Four countries from each of the top, middle, and bottom groups of the baseline Katz–Bonacich ranking • Computed with $\phi = 0.9/\lambda_{\max}(\mathbf{A})$

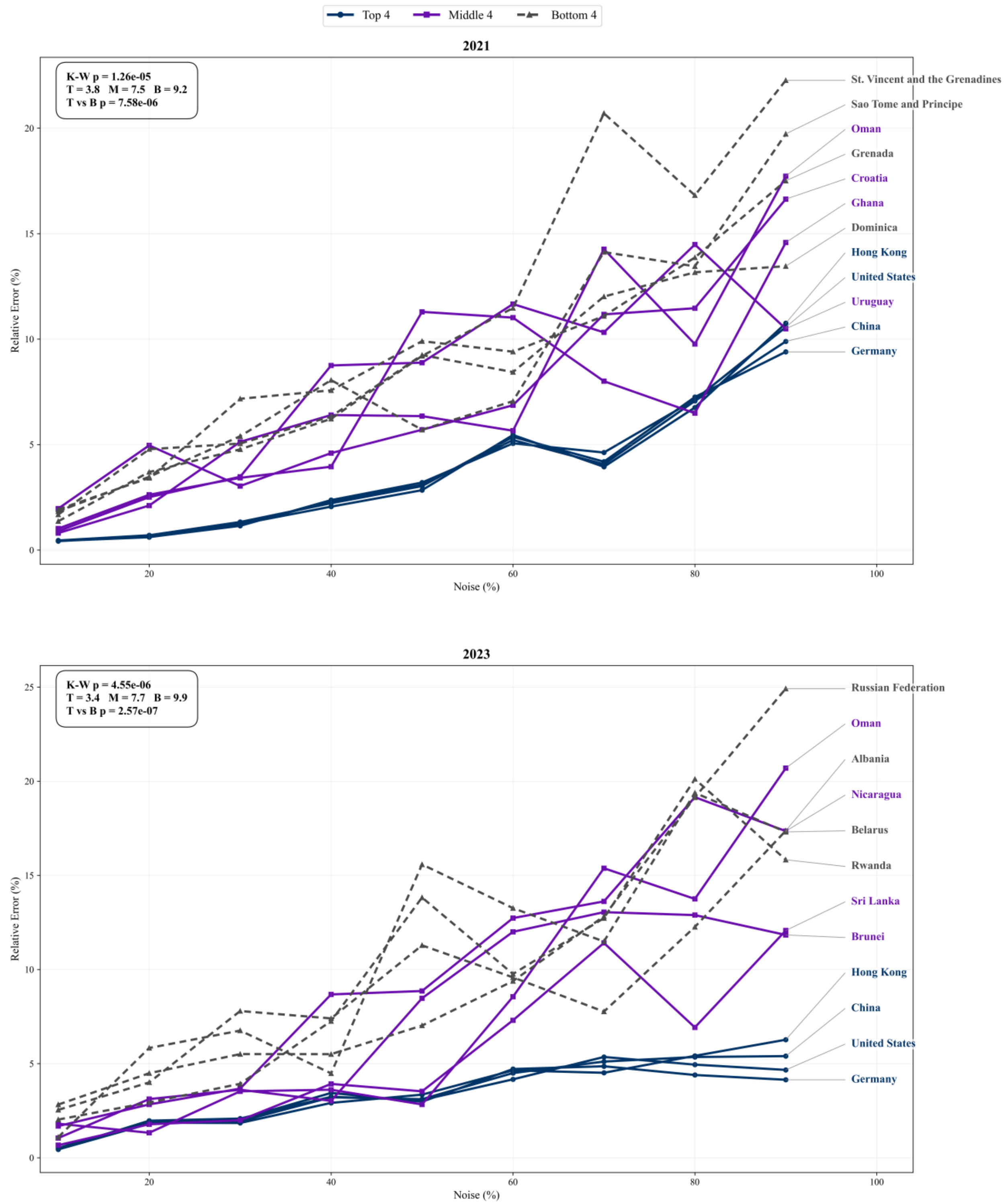

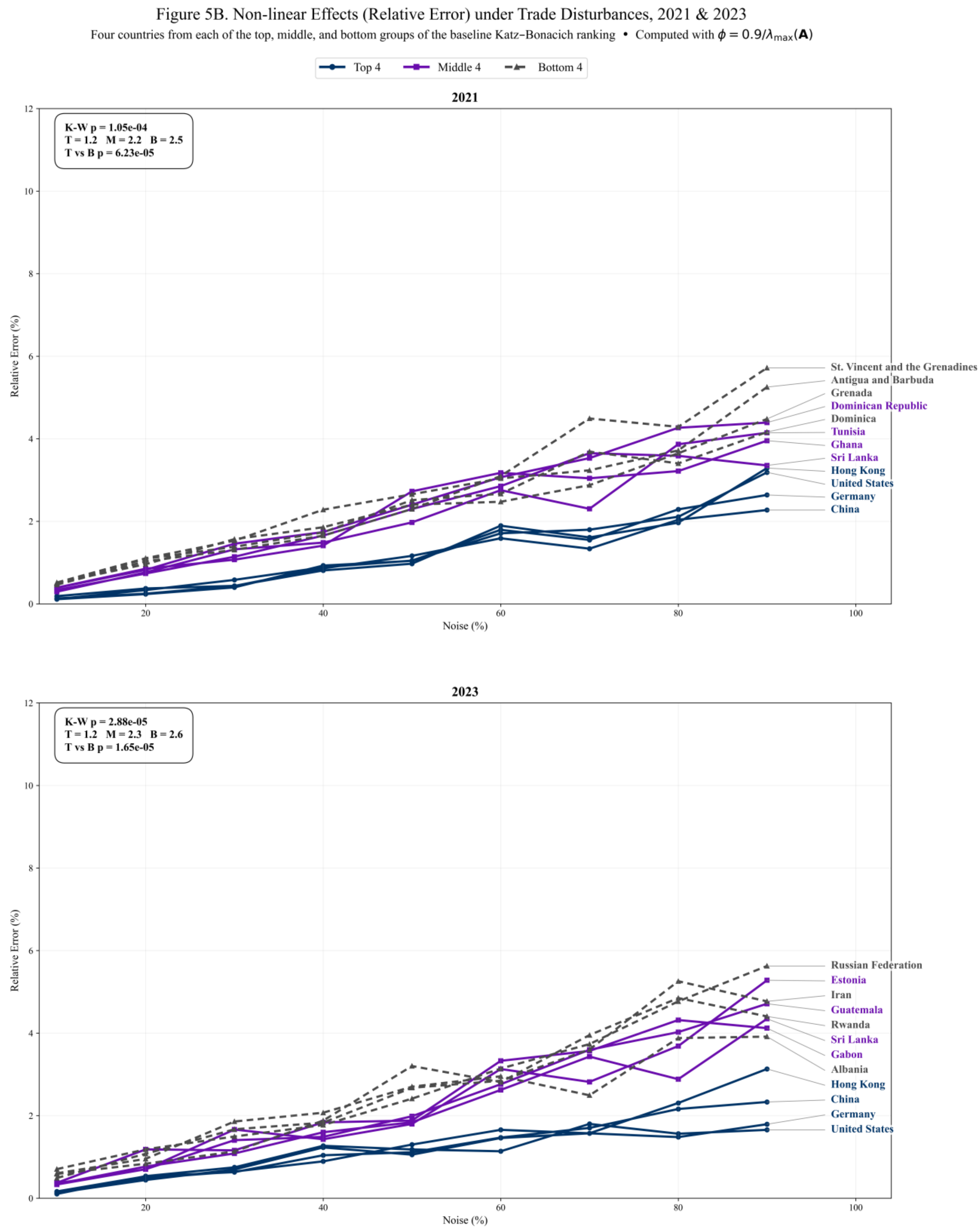

Figures 5A & 5B Relative error (%) in simulated Katz–Bonacich centrality as a function of disturbance intensity (noise-to-signal ratio, 10%–90%) for 2021 and 2023. Relative error measures the deviation of the simulated influence vector from its first-order linear approximation, capturing the magnitude of higher-order non-linear network effects. Four countries are selected from each of three groups defined by baseline centrality rank: top 4, middle 4, and bottom 4. Country labels on the right identify each trajectory. Figure 5A uses $\phi = 0.9/\lambda_{\max}(\mathbf{A})$; Figure 5B uses $\phi = 0.5/\lambda_{\max}(\mathbf{A})$. Bottom-ranked countries exhibit systematically larger and more volatile deviations as disturbances intensify, confirming that non-linear propagation effects disproportionately affect peripheral economies (H4). Statistical significance is assessed using Kruskal–Wallis and Mann–Whitney tests, reported in the inset boxes.

4.6 Methodological Implications of Robustness Analysis (H1–H4)

The robustness analysis yields several methodological implications for the study of weighted economic networks.

First, the positive association between baseline systemic influence and sensitivity shows that centrality measures are inherently position-dependent. Highly influential economies are more exposed to disturbances because their influence is generated through numerous direct and indirect export linkages. Measures such as MAIC (Mean Absolute Influence Change) provide a practical way to quantify how strongly a country's influence responds to shocks. Robustness assessments should therefore condition on baseline network position rather than treat sensitivity as homogeneous across countries.

Second, robustness is parameter-dependent. Changes in the propagation parameter ϕ alter the magnitude and transmission of influence responses even when the overall hierarchy remains stable. Empirical network analyses should therefore report sensitivity to alternative parameter values rather than rely on a single calibration.

Third, export concentration and systemic centrality capture distinct mechanisms of vulnerability. Concentration measures such as the Herfindahl–Hirschman Index reflect dependence arising from limited diversification across destination markets, whereas centrality measures capture amplification arising from network position and indirect spillovers. Distinguishing these channels is essential for identifying the underlying source of instability.

Fourth, deviations from the first-order approximation show that higher-order non-linear effects disproportionately affect lower-influence economies in proportional terms. Linear sensitivity analysis may therefore understate fragility among peripheral countries, even when their absolute changes in influence are modest.

Finally, the Stability–Influence Ratio (SIR) complements MAIC by relating baseline influence to volatility in simulated outcomes. While MAIC captures the average size of influence movements, SIR captures robustness relative to a country's baseline position. Because both measures are based on symmetric random variation, however, they do not fully capture vulnerability to targeted trade disruptions or strategic shocks. Robustness evaluation in economic networks should therefore combine diffuse disturbance analysis with structured stress-testing scenarios.

4.7 Shock Analysis (Trade reduction and redistribution)

We analyse how progressive reductions in U.S. export volumes affect the systemic influence of countries within the global export network. Influence rankings are derived from the network adjacency matrix under simulated reductions in U.S.-linked export flows ranging from 0.1% to 99%. The paper examines three country groups: a European bloc (United Kingdom, Germany, Italy, and France), a BRICS subset bloc (Russia, India, South Africa, and Brazil), and a subset of lower-influence peripheral economies (Morocco, Nigeria, Egypt, and Argentina). Simulations are performed separately for each year from 2016 to 2023.

In each simulation, bilateral trade flows involving the United States are reduced proportionally. However, only the exports that other countries previously sent to the United States are reallocated across the recipient bloc. The reduction in U.S. exports to foreign markets is treated as a direct contraction and is not redistributed. As a result, the model allows partial compensation through trade diversion, but not full replacement of the initial loss in trade flows.

To conserve space, the main text reports results for redistribution to the European bloc, while Appendix F presents quadratic and piecewise regression results for all recipient groups.

4.7.1: Shape of the Curve:

Hypothesis (H5a): Partial Compensation via Redistribution:

We hypothesise that partial reductions in U.S.-linked export flows generate a non-linear response in total network centrality due to the interaction between losses from a dominant hub and the redistribution of diverted exports to other economies. In particular, the simulations indicate a convex (U-shaped) relationship between the size of the U.S. export shock and aggregate Katz–Bonacich centrality. This expectation follows from two opposing forces. At low levels of disruption, losses from weaker linkages with the United States dominate and reduce aggregate centrality. At higher shock levels, redistributed export flows create new connections among recipient economies and partly offset these losses. When the propagation parameter is larger, these gains spread more strongly through indirect network channels, making recovery earlier and more pronounced. If the reduction in U.S. exports to foreign markets were also reallocated across recipient blocs, the contraction effect would be weaker and the response curve could take a different form. In that counterfactual case, redistribution gains could dominate at low or moderate shock levels, which could produce a concave (hump-shaped) relationship instead of the convex pattern observed here.

Let $v(r)$denote the Katz–Bonacich centrality vector of the shock-adjusted network and define total network centrality as $C(r) = 1^{\top} v(r)$. Moderate reductions in U.S.-linked export flows are initially associated with declines in total centrality, reflecting the dominant effect of weaker connections with the United States. As the shock intensifies, redistribution effects become stronger and the rate of decline weakens, with partial recovery in all years under the higher propagation regime. This pattern implies the existence of a turning point r^*, such that the marginal effect of the shock on $C(r)$is negative for $r \leq r^*$and positive for $r > r^*$. The simulation results are consistent with this theoretical expectation.

In the simulations, the interaction between export reductions and redistribution therefore produces a U-shaped relationship between total network centrality and shock size. This pattern remains robust across years and across alternative redistribution schemes. It is consistent with initial systemic losses followed by adjustment gains as redirected trade accumulates through the network. To characterise this simulated relationship more formally, we estimate the quadratic specification

$$C(r) = \alpha + \beta r + \gamma r^2 + u. \tag{26}$$

where $C(r)$denotes total Katz–Bonacich centrality and $r$is the percentage reduction in U.S.-linked export flows. This regression is used solely to characterise the simulated response function rather than to identify structural parameters.

The estimated coefficients confirm the presence of a positive turning point in every year of the sample. For $\phi = 0.5$, the threshold generally lies in the mid-seventies range. For $\phi = 0.9$, the threshold occurs earlier, typically in the mid-fifties to high-fifties range. Figures 6 illustrate these non-linear profiles. Across specifications, total network centrality declines under low and moderate shocks, reaches a minimum at the estimated threshold, and then recovers in every year when $\phi = 0.9$, with weaker recovery when $\phi = 0.5$ (Appendix F_1). Stronger propagation therefore lowers the shock level at which aggregate centrality reaches its minimum and recovery begins.

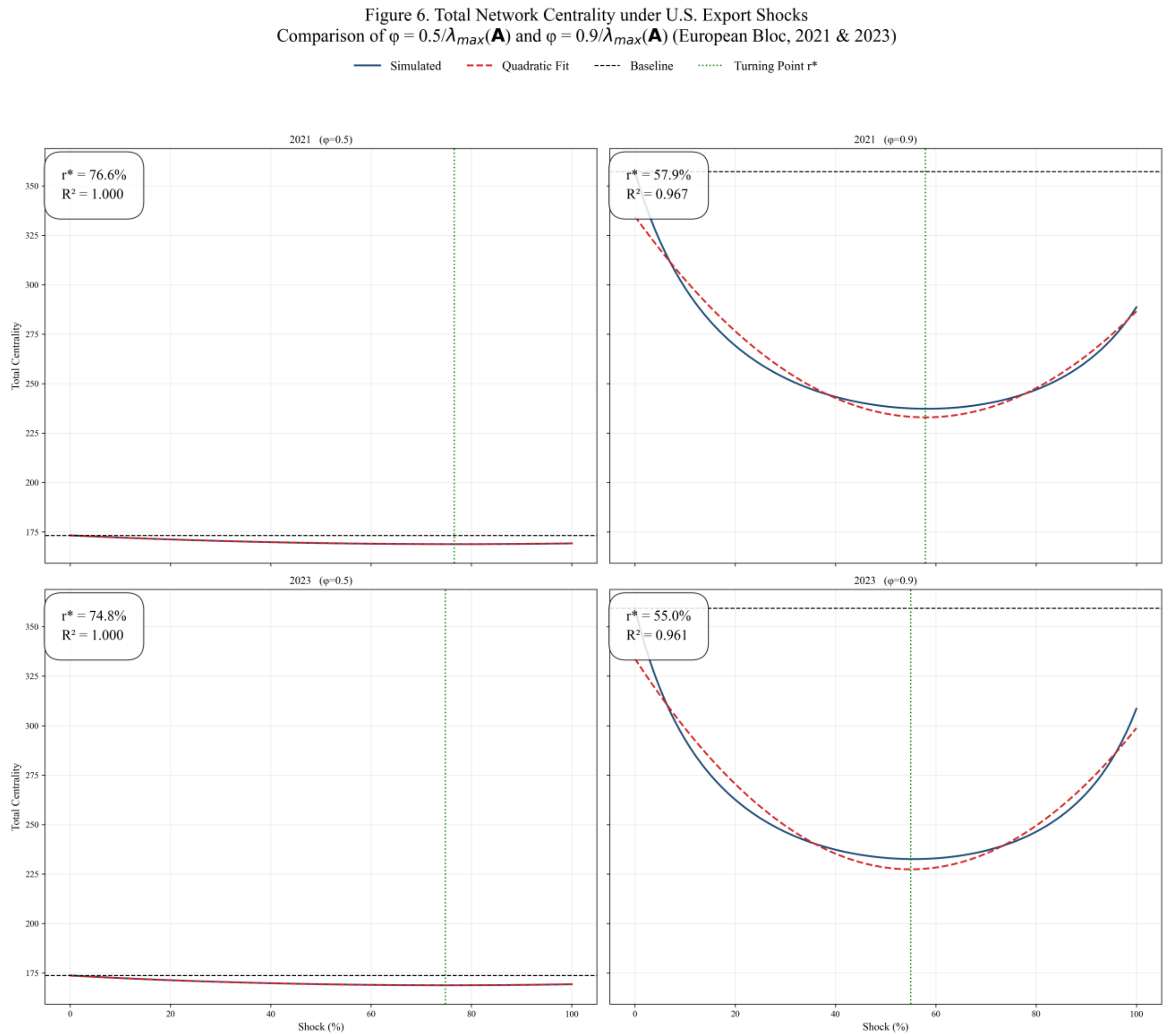

Figure 6 Simulated total Katz–Bonacich centrality of the global export network as a function of progressive reductions in U.S.-linked export flows (0%–100%), under two propagation regimes ($\phi = 0.5/\lambda_{\max}(\mathbf{A})$and $\phi = 0.9/\lambda_{\max}(\mathbf{A})$) for 2021 and 2023. Displaced exports are reallocated bilaterally among four European economies (France, Germany, Italy, United Kingdom) using weights proportional to internal export activity. The solid blue line shows the simulated centrality path; the dashed red line shows the fitted quadratic regression; the dashed black line marks baseline (pre-shock) centrality; and the green dotted vertical line identifies the estimated turning point r*,

the shock level at which aggregate centrality reaches its minimum. Under $\phi = 0.9/\lambda_{\max}(\mathbf{A})$,the turning point falls in the mid-to-high fifties range; under $\phi = 0.5/\lambda_{\max}(\mathbf{A})$it occurs later, in the mid-seventies range. The U-shaped response confirms H5a: moderate shocks reduce aggregate connectivity as hub losses dominate, while larger shocks trigger partial recovery as redistribution effects strengthen through indirect network channels.

Figures 7 and 8 visualise the network reconfiguration and country-level rank effects generated by these shocks.

Figure 7A. Before vs After U.S. Export Shock (2023, $\phi = 0.9/\lambda_{max}(\mathbf{A})$)

(a) Baseline Export Network (2023)

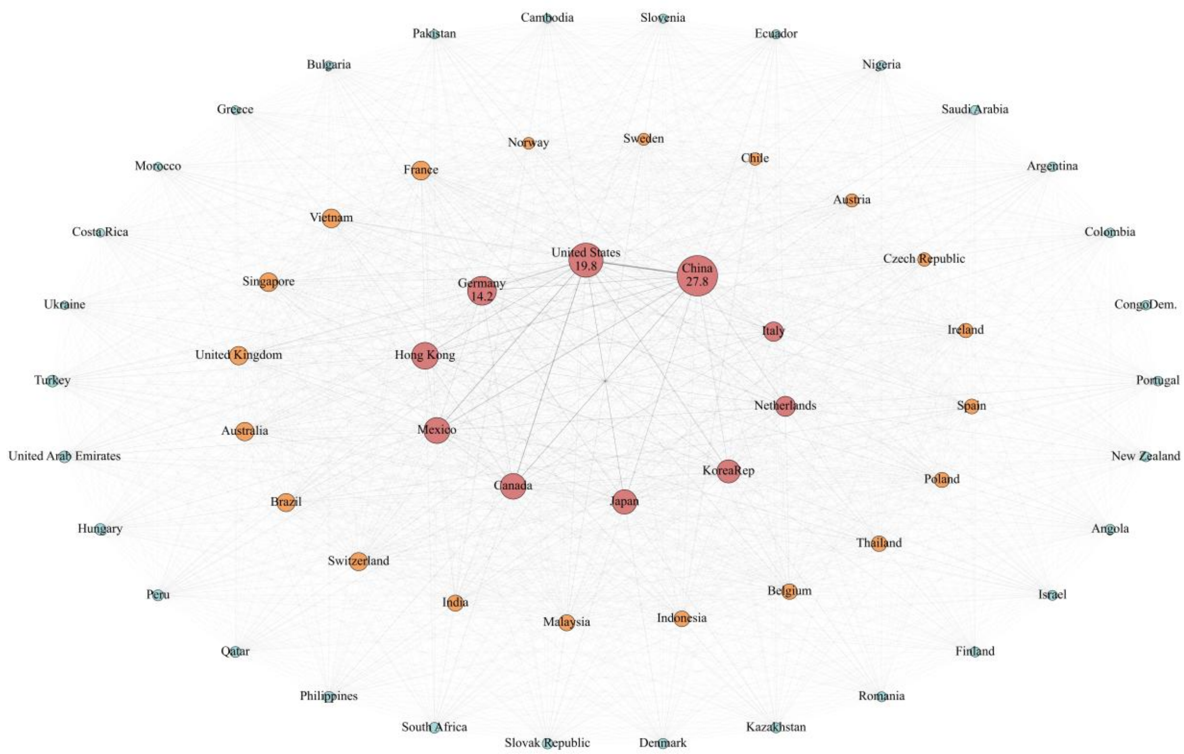

(b) After U.S. Export Shock (10.00%)

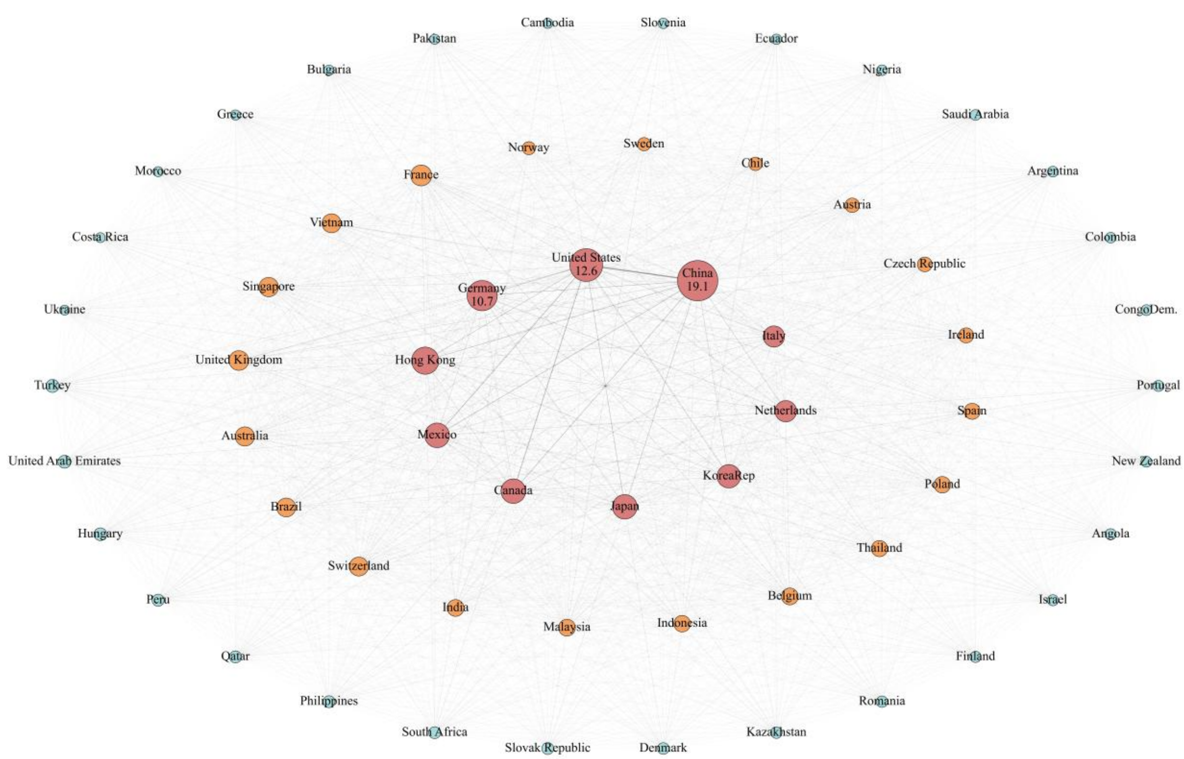

Figure 7B. Before vs After U.S. Export Shock (2023, $\phi = 0.5/\lambda_{max}(\mathbf{A})$)

(a) Baseline Network (2023)

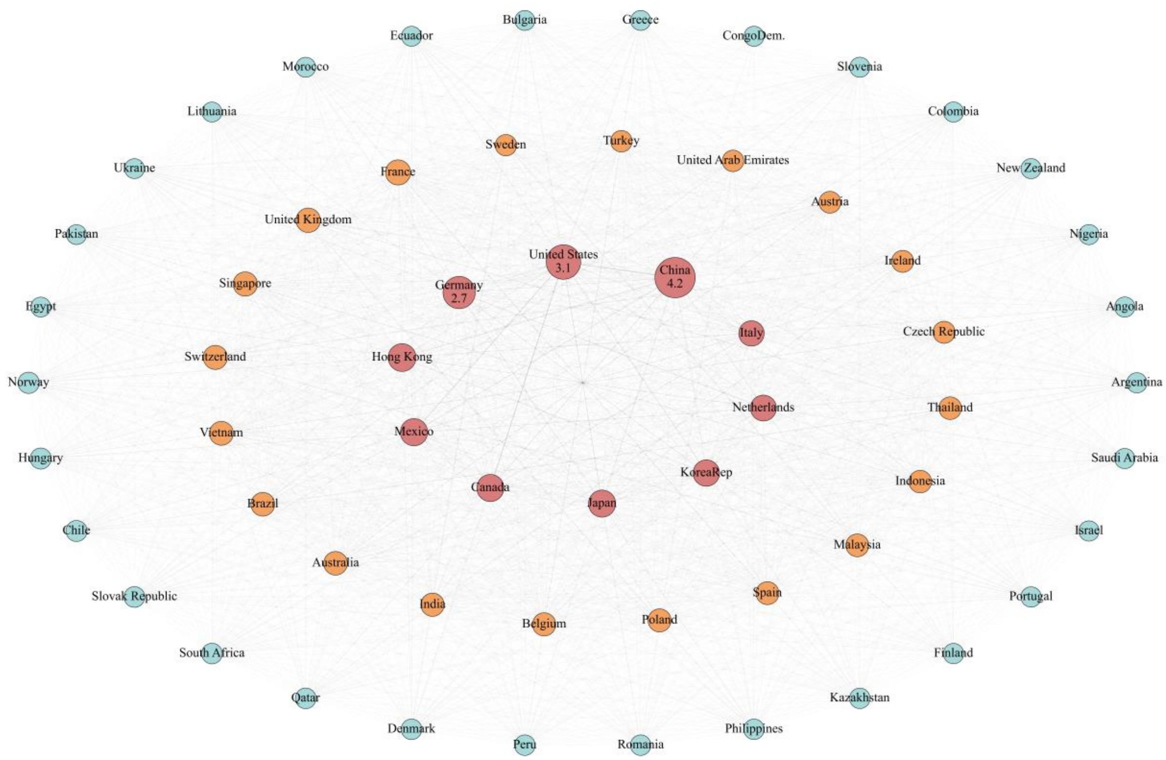

(b) After U.S. Export Shock (10.00%)

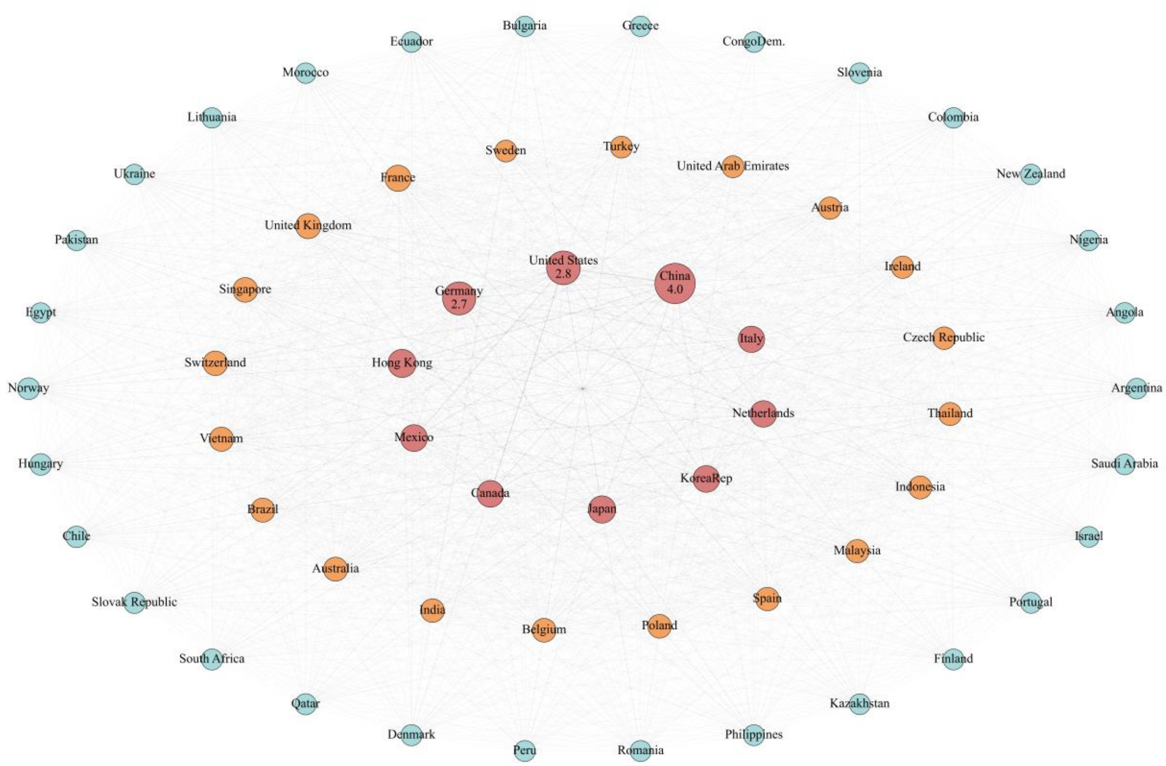

Figures 7 compares the global export influence network before and after a 10% percent reduction in U.S.-linked export flows in 2021 ($\phi = 0.9/\lambda_{\max}(\boldsymbol{A})$) and ($\phi = 0.5/\lambda_{\max}(\boldsymbol{A})$) the estimated turning point for the European redistribution bloc. Node size represents Katz–Bonacich centrality. For clarity of visualisation, Figure 7 illustrates the network structure for the top 60 countries in the baseline network.

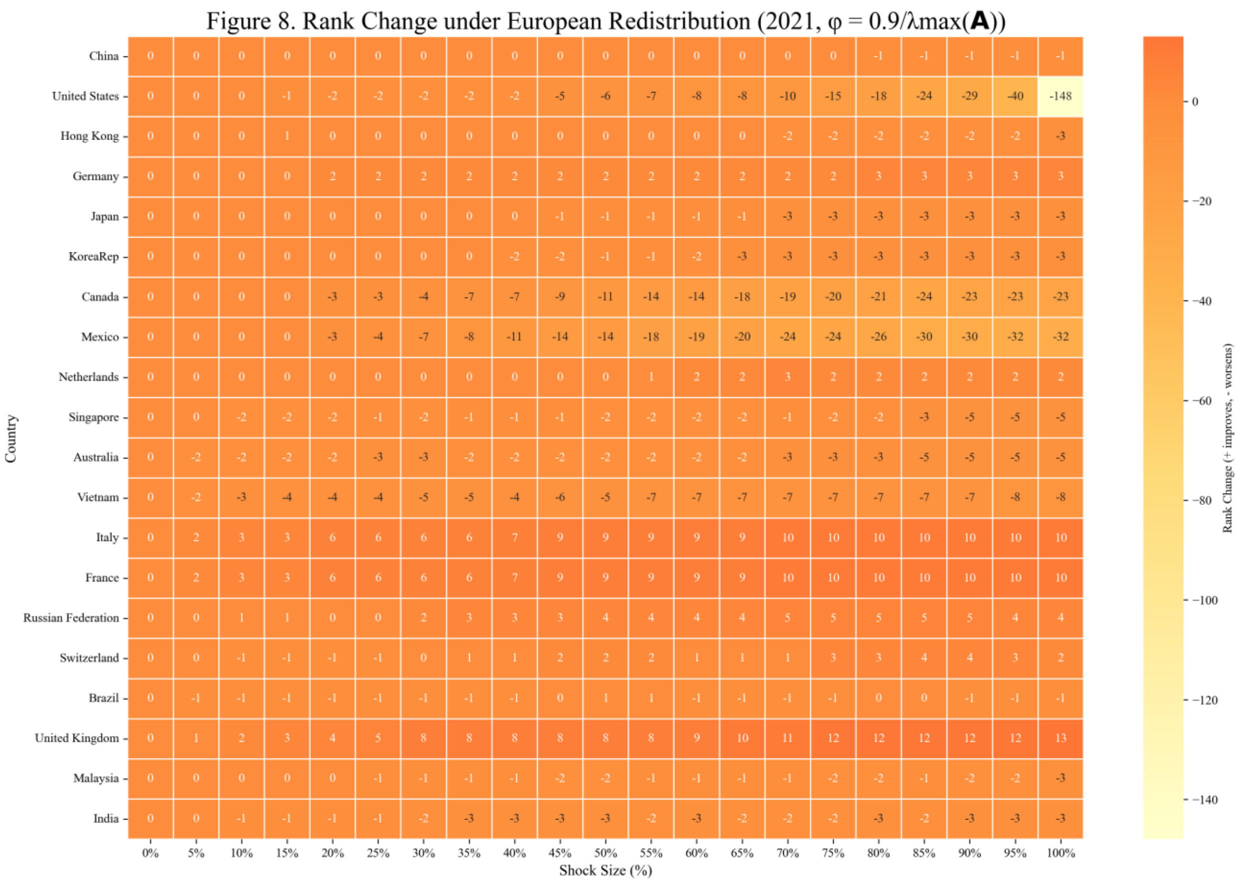

Figure 8. To conserve space, rank change for the top 20 baseline Katz–Bonacich economies under European redistribution (2021, ($\phi = 0.9/\lambda_{\max}(\boldsymbol{A})$). Positive = improvement; negative = decline.

4.7.2: Magnitude of Influence Responses

Simulation results indicate that reductions in U.S. export linkages generate an immediate decline in systemic influence across all bloc configurations. Even moderate shocks reduce total network centrality because the United States functions as a highly connected hub in the global trade system. The initial loss of connectivity from bilateral trade contraction exceeds the gains from redirected flows within recipient blocs.

The magnitude and persistence of this decline differ across blocs. The European bloc experiences a smaller contraction and a stronger recovery at higher shock levels, consistent with its dense internal trade structure and multiple alternative transmission channels. The BRICS subset and lower-influence emerging-economy bloc exhibit larger and more persistent losses, with weaker rebound effects. In these cases, redistribution partly offsets the shock but does not restore baseline systemic influence.

As a result, economies embedded in dense and diversified trade networks remain more resilient than blocs with lower internal connectivity, but no group is fully insulated from trade disruption. These findings indicate that, under realistic shock magnitudes, the systemic costs of weaker trade with the United States exceed the benefits of redistribution, while internal bloc structure determines the extent of subsequent adjustment.

4.7.3: Threshold Effect in aggregate Centrality (H5b)

Hypothesis H5b proposes a threshold effect in the relationship between trade shocks and systemic centrality. Aggregate centrality is expected to decline for small to medium reductions in U.S. exports because losses from the highly central U.S. economy initially exceed the gains from redirected trade. Beyond a critical level of disruption, the marginal decline is expected to weaken, and in some cases partial recovery may emerge as redirected flows improve connectivity elsewhere in the network.

To test this hypothesis, we estimate a piecewise specification that allows the marginal effect of shocks to differ before and after a threshold level r^*:

$$C(r) = \alpha + \beta_1 r \mathbf{1}\{r \leq r^*\} + \beta_2 r \mathbf{1}\{r > r^*\} + u. \tag{27}$$

where $1\{\cdot\}$is an indicator function. The coefficients $\beta_1$and $\beta_2$capture the slope of the response below and above the threshold, respectively. A change in slope across regimes indicates non-linearity in the relationship between shocks and aggregate centrality.

The implied threshold is given by:

$$r^* = -\frac{\beta_1}{2\beta_2}. \tag{28}$$

where r^*identifies the shock magnitude at which aggregate centrality reaches its minimum or changes slope.

The results show a consistent non-linear pattern across all three blocs. Under the higher propagation setting ($\phi = 0.9/\lambda_{\max}(\boldsymbol{A})$), centrality declines sharply at low shock levels, reaches an interior turning point, and then partially recovers after redistribution effects strengthen. Under the lower propagation setting ($\phi = 0.5/\lambda_{\max}(\boldsymbol{A})$), the decline is flatter and recovery effects are substantially weaker, which indicates that indirect transmission is more limited when network amplification is lower.

Across specifications, the European bloc reaches its turning point at lower shock magnitudes than the BRICS subset and the lower-influence emerging-economy bloc. This result suggests that blocs with denser internal trade linkages adjust more rapidly through internal reallocation, while less connected blocs require larger disruptions before redistribution effects become more important. Across the BRICS subset and lower-influence emerging-economy bloc, threshold timing varies across years, indicating that turning points depend not only on bloc membership but also on changes in internal network composition and the presence of major hub economies.

The timing of bloc-level adjustment can be interpreted with a series expansion of the influence response:

$$\Delta v(r) = \sum_{k=1}^{\infty} \phi^k \, (\boldsymbol{R}_r \boldsymbol{A}^{k-1})\boldsymbol{1}. \tag{29}$$

This expression shows that the total response consists of successive rounds of transmission through the network. The first term captures the immediate effect of redistributed trade, while higher-order terms capture indirect spillovers through longer trade paths.

Since $\Delta v(r)$is a vector, its i-th entry satisfies:

$$\Delta v_i(r) = \underbrace{\phi \sum_j \boldsymbol{R_{ij}}(r) +}_{\text{the direct effect}} \underbrace{\phi^2 \sum_{j,k} \boldsymbol{R_{ij}}(r)\boldsymbol{A_{ik}} + \phi^3 \sum_{j,k,l} \boldsymbol{R_{ij}}(r)\boldsymbol{A_{jk}}\boldsymbol{A_{kl}} + \dots}_{\text{indirect effects}}. \tag{30}$$

The decomposition shows that blocs with stronger internal connectivity benefit earlier from higher-order spillovers, which helps explain why the European bloc reaches its turning point sooner than the alternative recipient groups. Proof: See Appendix G.

The estimated response functions for total network centrality reveal a consistent non-linear pattern across all three blocs (Figures 9A and 9B). Under the higher propagation setting ($\phi = 0.9/\lambda_{\max}(\boldsymbol{A})$), total network centrality declines sharply at low shock levels, reaches an interior turning point, and then partially recovers as redistribution effects strengthen. The recovery is most pronounced for the European bloc, whose curve turns upward earlier and more strongly than the alternatives.

Under the lower propagation setting ($\phi = 0.5/\lambda_{\max}(\mathbf{A})$), the response curves are substantially flatter (Figure 9B). Centrality still declines as shocks intensify, but recovery effects are weaker or absent within the simulated range, indicating that indirect transmission is more limited when network amplification is low.

Across specifications, the European bloc reaches its turning point at lower shock magnitudes than the BRICS subset and the lower-influence emerging-economy bloc (Figure 9A). This pattern suggests that blocs with denser internal trade linkages adjust more rapidly through internal reallocation, while less connected blocs require larger disruptions before redistribution effects become more important. By contrast, the later or weaker turning points for the alternative recipient groups indicate lower absorptive capacity and fewer indirect channels through which redirected trade can generate system-wide gains. Figures 9A and 9B show that bloc composition and the propagation parameter jointly shape adjustment dynamics.

Figure 9A. Systemic Effects of Trade Redistribution: Europe, BRICS, and South ($\varphi = 0.9/\lambda\max(\mathbf{A})$), 2021 & 2023

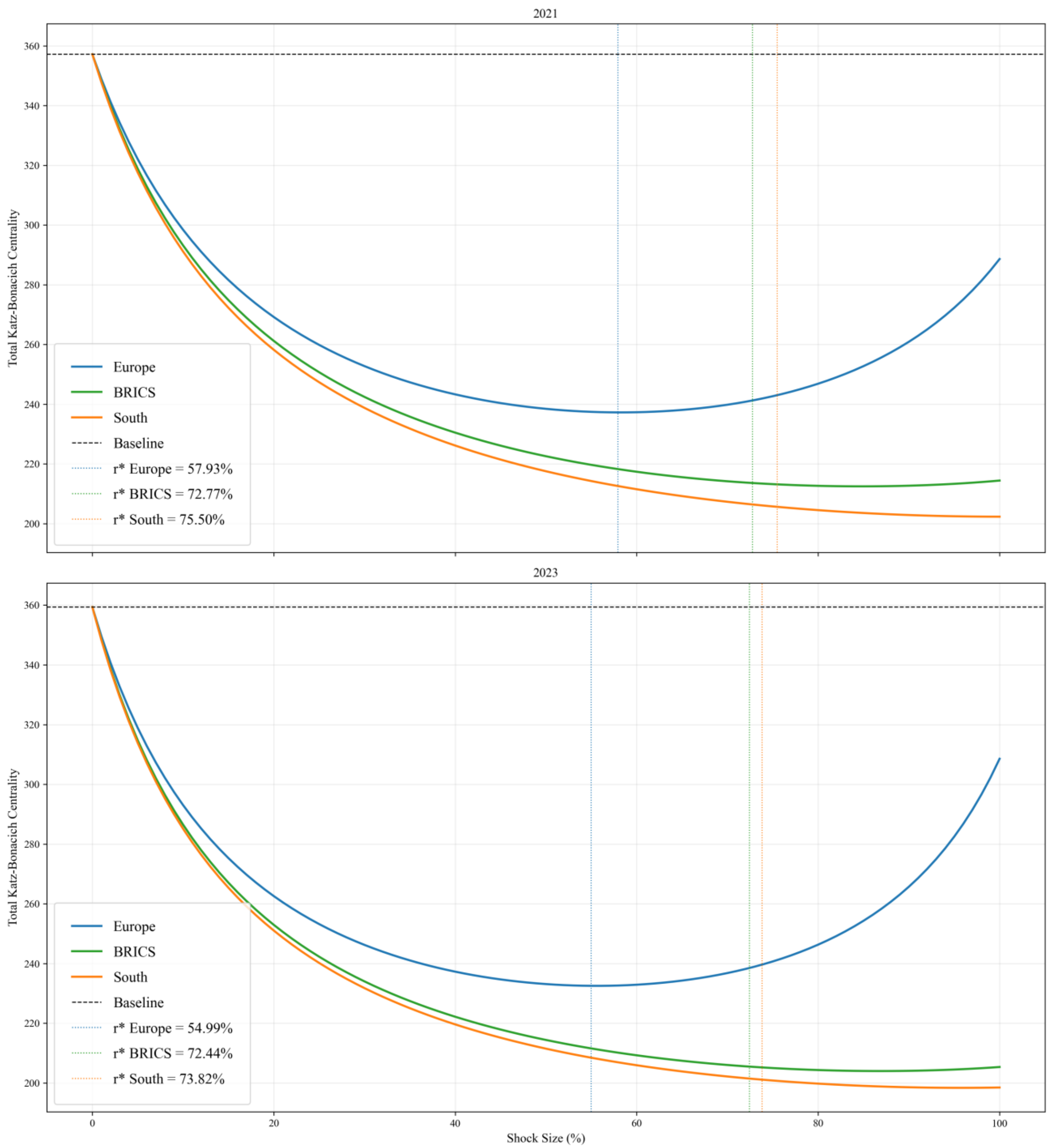

Figure 9B. Systemic Effects of Export Redistribution: Europe, BRICS, and South ($\varphi = 0.5/\lambda\max(\mathbf{A})$), 2021 & 2023

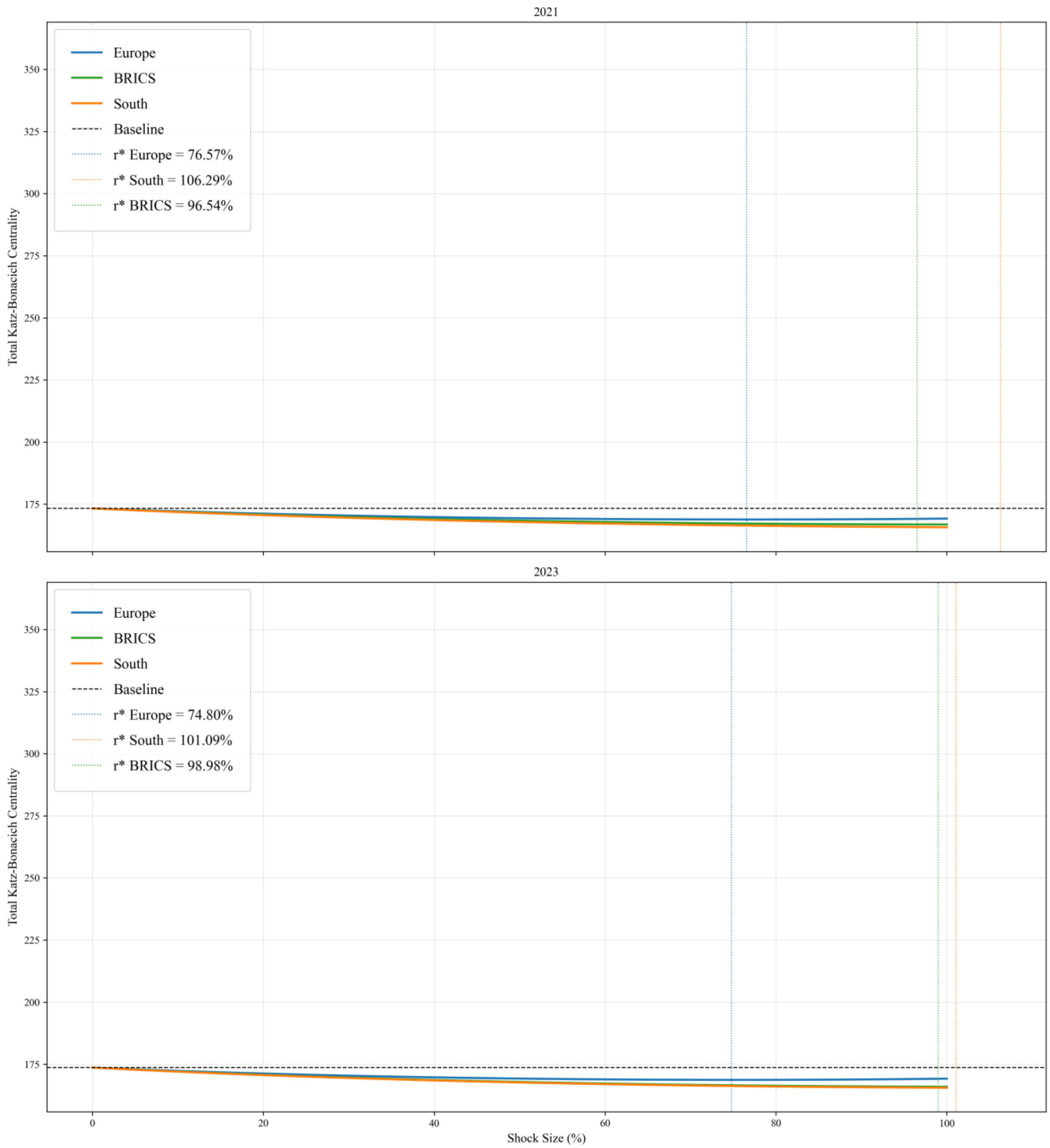

Figures 9A & 9B Simulated total Katz–Bonacich centrality of the global export network as a function of progressive reductions in U.S.-linked export flows (0%–100%) for 2021 and 2023, comparing three alternative recipient blocs: a European bloc (France, Germany, Italy, United Kingdom), a BRICS subset (Russia, India, South Africa, Brazil), and a lower-influence peripheral bloc (Morocco, Nigeria, Egypt, Argentina). Coloured dotted vertical lines mark each bloc's estimated turning point $\boldsymbol{r}^*$. Figure 9A uses ($\phi = 0.9/\lambda_{\max}(\mathbf{A})$; Figure 9B uses ($\phi = 0.5/\boldsymbol{\lambda}_{\mathbf{max}}(\mathbf{A})$). Under the higher propagation regime, the European bloc reaches its turning point at lower shock levels than the BRICS and peripheral blocs, reflecting denser internal trade linkages and stronger indirect transmission channels. Under the lower propagation regime, recovery effects are substantially weaker or absent across all blocs. Across specifications, trade shocks redistribute systemic influence before reducing aggregate connectivity, with the magnitude and timing of adjustment shaped jointly by bloc composition and the propagation parameter.

4.7.6: Methodological Reflection

The results provide three methodological insights.

First, they validate the theoretical mechanism in an empirically tractable setting. The analytical framework implies that the effect of U.S.-linked export reductions on aggregate network centrality reflects two offsetting forces: a negative effect associated with contraction in trade involving a highly central hub, and a positive effect generated by the reallocation of displaced exports through alternative partners. Although this decomposition does not impose a specific global functional form, it provides micro-foundations for non-linear aggregate responses. Hypothesis H5a translates this mechanism into a testable prediction. The simulations generate systematic non-linear responses, with initial declines in centrality followed by attenuation or partial recovery as reallocation effects strengthen. Estimating a quadratic specification provides a tractable way to recover the turning point, $r^* = -\beta/(2\gamma)$, at which losses are maximised or begin to moderate.

Second, the observed non-linearity is not an artefact of a particular parameterisation. Robustness checks using alternative values of the propagation parameter ϕ produce qualitatively similar response profiles, although the magnitude of effects and the location of turning points vary across specifications. Threshold behaviour therefore appears to be a structural property of the network rather than a consequence of any single calibration.

Third, the findings illustrate the gains from combining formal network models with reduced-form estimation. Theory disciplines the expected response shape, while quadratic and threshold regressions provide directly estimable summaries of simulated outcomes. This yields a general empirical framework for analysing export adjustment in interconnected systems where shocks propagate through indirect network channels rather than solely through bilateral exposures.

More broadly, the analysis shows how network trade models can be translated into empirically testable non-linear hypotheses, offering a template for applied work that moves beyond linear or purely bilateral intuition.

The analytical scope of the framework is extended further in Appendices H and I. Appendix H generalises the benchmark simulations by allowing outcomes to vary with recipient set size and the degree of successful reallocation, thereby relaxing the fixed bloc assumption used in the main exercises. Appendix I recasts redistribution as a network design problem in which displaced trade is allocated to maximise aggregate connectivity after a shock. These extensions show that the framework is not confined to the specific simulations reported in the main text, but can be applied to broader structural and policy questions.

5. Discussion and Policy Implications

5.1 Systemic Influence, Volatility, and Structural Vulnerability

The results establish a structural trade-off between systemic influence and stability in global export networks. Economies that occupy highly central positions derive influence from extensive direct and indirect trade linkages, but this centrality also increases sensitivity to disturbances. The positive association between baseline influence and volatility indicates that systemic importance and exposure are jointly determined by network position. Economies that transmit shocks widely through the network face greater exposure to fluctuations in trade conditions.

This finding refines how economic power should be interpreted in interconnected systems. Highly influential economies such as the United States and China possess broad structural reach, but they are not insulated from instability. Their central role means that even modest disturbances generate comparatively large changes in measured influence. More peripheral economies often display lower absolute volatility, although relatively small absolute changes may still produce sizeable proportional movements in influence.

Trade concentration introduces a distinct source of vulnerability. Economies whose exports are concentrated among a narrow set of partners remain highly exposed to partner-specific shocks, whereas diversified economies distribute risk across a broader portfolio of trade relationships. Concentration effects also interact with baseline centrality. Strong systemic embeddedness amplifies fluctuations even where diversification is relatively high. Structural position and portfolio concentration therefore represent separate but interacting channels of vulnerability.

Countries that seek to reduce structural vulnerability should focus not only on expanding trade volume, but also on diversifying export destinations and reducing excessive dependence on single hub markets. Policies that broaden market access, deepen regional integration, and strengthen alternative trade corridors improve resilience by limiting exposure to partner-specific disruptions. This logic is increasingly visible in policy debates. Recent statements by Canadian Prime Minister Mark Carney[3] that excessive reliance on the U.S. market has become a structural weakness, Mexico's efforts[4] to reduce dependence on U.S. natural gas imports, and Japanese Prime Minister Sanae Takaichi's[5] warning in March 2026 that placing all eggs in the U.S. basket is probably not wise following the exposure of Japan's structural energy vulnerability through the Strait of Hormuz crisis, illustrate how governments across the income and development spectrum reassess concentration risk and diversification strategies in practice.

From a methodological perspective, the findings show that symmetric stochastic robustness measures capture resilience to diffuse uncertainty but understate vulnerability to targeted disruptions. Indicators such as the Stability-Influence Ratio are informative for measurement noise and unsystematic volatility, yet they do not capture exposure to deliberate trade restrictions, sanctions, or strategic decoupling. A fuller assessment of systemic vulnerability therefore requires combining diffuse disturbance analysis with targeted shock simulations.

In geopolitical terms, economic centrality confers both leverage and exposure. States that seek systemic influence through trade integration must also manage the instability associated with highly connected positions. Selective disengagement may lower volatility, but it does so at the cost of diminished systemic relevance. Influence and stability are therefore jointly shaped by network

[3] See The Guardian (20 April 2026), "Mark Carney says Canada-U.S. economic ties now a weakness."
[4] See The Independent / AP (8 April 2026), "Mexico's president weighs fracking to curb reliance on U.S. natural gas."
[5] See Nakano (2026) and Carbon Brief (2026). Takaichi warned at the White House summit on 19 March 2026 that placing all eggs in the U.S. basket is probably not wise, a reaction to Japan's acute exposure to energy supply disruption through the Strait of Hormuz

structure. These findings are consistent with the first-order sensitivity result in Proposition 1 and its structural interpretation under trade concentration in Proposition 2.

5.2 Redistribution, Threshold Effects, and Economic Statecraft

The shock simulations show that reductions in trade involving a dominant hub economy do not map linearly into systemic outcomes. Aggregate centrality declines following the initial contraction in U.S.-linked exports because hub contraction losses dominate the gains from redistribution. As the shock intensifies, redistribution effects strengthen and the rate of decline slows. Only beyond the estimated turning point r^* do redirected trade flows accumulate sufficiently through the network to generate partial recovery in aggregate centrality. This non-linear response reflects the interaction between the negative effects of hub contraction and the positive effects of network adjustment, and it cannot be recovered from bilateral trade data alone.

The turning point r^* provides a useful benchmark within the model environment. It identifies the shock magnitude at which aggregate losses stop intensifying and network adjustment effects begin to dominate. Below this threshold, hub contraction dominates and centrality falls despite ongoing redistribution. Beyond it, redirected flows strengthen secondary hubs and partial recovery becomes possible, although outcomes remain sensitive to recipient capacity, network structure, and the degree of successful reallocation.

Redistribution generates clear distributional asymmetries. Gains from diverted trade accrue disproportionately to economies that are already well connected, while more peripheral economies benefit only through indirect spillovers. Trade shocks therefore reallocate influence more often than they eliminate it. Economies with highly concentrated export dependence on a dominant partner experience the largest direct losses when that relationship contracts.

These findings carry direct implications for sanctions, tariffs, and other forms of economic statecraft. Policies intended to weaken a rival's systemic position must account for the threshold dynamic identified in the simulations. Moderate restrictions reduce overall connectivity but do not strengthen alternative hubs, because below r^*hub contraction losses exceed redistribution gains. Only large and sustained disruptions push the system beyond the turning point, at which stage redirected flows begin to consolidate influence among secondary powers. The effectiveness of trade interventions therefore depends critically on whether the shock is sufficient in scale and persistence to cross this threshold.

For policymakers, this implies that the impact of sanctions or tariff measures cannot be assessed through bilateral trade losses alone. Successful intervention requires that alternative partners lack the capacity to absorb displaced trade and that targeted economies cannot reroute flows through third countries. Measures aimed at reducing strategic dependence may therefore require coordination across allied economies and complementary policies that limit circumvention channels.

The results show more broadly that trade policy affects systemic power through reallocation as well as contraction. Third countries absorb and transmit displaced flows and reshape influence patterns across the wider system. In an increasingly multipolar trading environment, economic statecraft operates within a network in which influence is redistributed across nodes rather than simply removed from the system.

6. Conclusions

This paper examines how shocks to a dominant hub economy propagate through the global trade network and how the redistribution of displaced trade flows reshapes systemic influence. The analysis combines robustness assessment under symmetric random trade disturbances with policy-relevant trade redistribution scenarios. The results clarify the interaction between network structure, trade concentration, and influence volatility, and identify structural mechanisms within the trade system. These results should not be interpreted as direct forecasts of specific sanctions or trade conflicts. The empirical results in the main text rely on export networks. Although the framework applies symmetrically to import networks, reporting both sets of results would substantially increase the length of the paper and dilute the central mechanisms under study.

The paper introduces two novel metrics. The Stability–Influence Ratio relates a country's baseline systemic importance to the volatility of that importance under simulated disturbances, and the Mean Absolute Influence Change measures the average magnitude of influence responses across shock scenarios. These metrics fill a gap that standard centrality measures cannot address: they distinguish robust systemic importance from fragile prominence and quantify how strongly a country's network position responds to trade uncertainty. The United States and China occupy the two most central positions in the baseline network, yet they also exhibit disproportionate responsiveness to shocks. Smaller and less diversified economies display high relative volatility even when their baseline influence is modest. Systemic influence and instability are therefore structurally linked rather than independent properties.

Trade redistribution generates a non-linear response in aggregate network centrality. Initial reductions in United States-linked trade lower total centrality because hub contraction losses dominate the gains from redistribution. As the shock intensifies, redistribution effects strengthen and the rate of decline slows. Beyond the estimated turning point r*, redirected trade flows toward alternative well-connected economies begin to offset hub losses and aggregate centrality partially recovers. Systemic influence is therefore reallocated before any durable reduction in aggregate connectivity occurs.

Trade concentration, measured using the Herfindahl-Hirschman Index, plays a central role in shaping sensitivity to disturbances. Economies with concentrated trade portfolios experience larger absolute changes in influence under shocks. Highly central hubs remain volatile regardless of diversification because their systemic position amplifies transmitted disturbances. Network centrality and trade concentration operate through distinct but complementary channels in generating instability.

Network topology and the propagation parameter condition the amplification of shocks. Higher responsiveness magnifies fluctuations for central nodes, while peripheral nodes exhibit more moderate absolute responses but larger proportional deviations. Higher-order non-linear effects are most pronounced for lower-ranked economies, which underscores the limits of first-order approximations in assessments of systemic vulnerability.

The findings carry both methodological and policy implications. Policies that target dominant trade hubs generate non-linear systemic effects. Below the estimated threshold r*, hub contraction dominates and aggregate centrality declines despite ongoing redistribution toward alternative partners. Only beyond this threshold do redirected trade flows accumulate sufficiently through the network to generate partial recovery. Trade restrictions therefore reshape systemic influence before they materially weaken aggregate connectivity, and their full systemic consequences cannot be read from bilateral exposure alone.

In the context of contemporary trade conflicts and economic fragmentation, moderate trade restrictions reduce aggregate network centrality because hub contraction losses exceed the gains from redistribution at low shock levels. Only large and sustained disruptions push the system beyond the turning point, at which stage redirected trade flows strengthen alternative hubs and partial systemic recovery becomes possible. Strategic trade interventions must therefore account for this threshold dynamic. Efforts to diminish a rival's systemic position through moderate restrictions are unlikely to consolidate influence among secondary powers as they simply reduce overall connectivity. Sufficient scale and persistence are necessary conditions for redistribution effects to dominate and for alternative hubs to gain meaningfully.

Economies with concentrated trade structures remain vulnerable even under limited disruptions. Trade wars do not affect all countries symmetrically. Highly diversified hubs absorb shocks through broader adjustment channels, whereas concentrated economies experience sharper losses in systemic influence.

Two extensions follow naturally from this framework. First, future work could allow contraction rates to vary across trading partners as a function of systemic importance, so that disruptions involving highly central economies generate larger effective losses than shocks to peripheral nodes. This would endogenise the contraction mechanism itself within the network structure that this paper identifies as central. Second, the framework could be applied to financial networks, where links represent portfolio exposures, bank claims, or liquidity provision. In that setting, the model would complement standard factor approaches by tracing how systemic importance and indirect connections shape shock transmission, a question this paper shows to be empirically consequential in trade networks.

Power in the world economy is not a fixed attribute of dominant states. It is an emergent property of network structure, and it is continuously reconfigured whenever trade flows are disrupted, redirected, or rebuilt. In an increasingly fragmented world economy, understanding who gains, who loses, and when systemic losses begin to dominate requires a network perspective rather than a bilateral one.

References:

Acemoglu, D., Carvalho, V.M., Ozdaglar, A. & Tahbaz-Salehi, A. (2012). The network origins of aggregate fluctuations. *Econometrica*, 80(5), pp.1977–2016.

Acemoglu, D., Ozdaglar, A. & Tahbaz-Salehi, A. (2015). Systemic risk and stability in financial networks. *American Economic Review*, 105(2), pp.564–608.

Alatriste Contreras, M.G. & Fagiolo, G. (2014). Propagation of economic shocks in input–output networks: A cross-country analysis. *Physical Review E*, 90(6), 062812.

Ballester, C., Calvó-Armengol, A. & Zenou, Y. (2006). Who's who in networks. Wanted: the key player. *Econometrica*, 74(5), pp.1403–1417.

Baqaee, D.R. & Farhi, E. (2019). The macroeconomic impact of microeconomic shocks: Beyond Hulten's theorem. *Econometrica*, 87(4), pp.1155–1203.

Barrot, J.-N. & Sauvagnat, J. (2016). Input specificity and the propagation of idiosyncratic shocks in production networks. *Quarterly Journal of Economics*, 131(3), pp.1543–1592.

Beck, K. & Jackson, K. (2024). International trade fluctuations: Global versus regional factors. *Canadian Journal of Economics*, 57, pp.331–358.

Boehm, C.E., Flaaen, A. & Pandalai-Nayar, N. (2019). Input linkages and the transmission of shocks: Firm-level evidence from the 2011 Tōhoku earthquake. *Review of Economics and Statistics*, 101(1), pp.60–75.

Boldi, P. & Vigna, S. (2014). Axioms for centrality. *Internet Mathematics*, 10(3–4), pp.222–262.

Borgatti, S.P., Carley, K.M. & Krackhardt, D. (2006). On the robustness of centrality measures under conditions of imperfect data. *Social Networks*, 28(2), pp.124–136.

Bove, V., Di Salvatore, J. & Nisticò, R. (2023). Economic sanctions and trade flows in the neighbourhood. *Journal of Law and Economics*, 66(4), pp.671–697.

Brandes, U. & Fleischer, D. (2005). Centrality measures based on current flow. In V. Diekert & B. Durand (Eds.), *STACS 2005. Lecture Notes in Computer Science*, vol. 3404 (pp.533–544). Berlin: Springer.

Carvalho, V.M., Nirei, M., Saito, Y.U. & Tahbaz-Salehi, A. (2021). Supply chain disruptions: Evidence from the Great East Japan Earthquake. *Quarterly Journal of Economics*, 136(2), pp.1255–1321.

Cerina, F., Zhu, Z., Chessa, A. & Riccaboni, M. (2015). World input-output network. *PLOS ONE*, 10(7), e0134025.

Chaney, T. (2014). The network structure of international trade. *American Economic Review*, 104(11), pp.3600–3634.

Chen, S. (2025). International production networks and the propagation of financial shocks. *Journal of International Economics*, 153, 104039.

Dai, S., Ji, J. & Yu, H. (2026). Technology import and biased technological progress in transforming economies: Evidence from China. *Review of Development Economics*, 30(2), pp.1194–1214.

Debreu, G. & Herstein, I.N. (1953). Nonnegative square matrices. *Econometrica*, 21(4), pp.597–607.

De Benedictis, L. & Tajoli, L. (2011). The world trade network. *The World Economy*, 34(8), pp.1417–1454.

Elliott, M., Golub, B. & Jackson, M.O. (2014). Financial networks and contagion. *American Economic Review*, 104(10), pp.3115–3153.

Fagiolo, G., Reyes, J. & Schiavo, S. (2009). World-trade web: Topological properties, dynamics, and evolution. *Physical Review E*, 79, 036115.

Fan, Z., Long, R., Anwar, S. & Wang, J. (2025). Does centrality within trade agreements network matter to economic complexity? The conditioning effects of network structure. *International Review of Economics & Finance*, 98, 103892.

Garlaschelli, D. & Loffredo, M.I. (2005). Structure and evolution of the world trade network. *Physica A*, 355, pp.138–144.

Gavoille, N. (2025). A short drop or a sudden stop? Sanctions, trade shocks, and firms' adjustment margins. Latvijas Banka Working Paper No. 2025/03.

Ignatenko, A., Lashkaripour, A., Macedoni, L. & Simonovska, I. (2025). Making America great again? The economic impacts of Liberation Day tariffs. *Journal of International Economics*, 157, 104138.

Liu, X. & Zhang, Y. (2025). The nonlinear impact of trade policy uncertainty on corporate ESG performance. *International Review of Economics & Finance*, 103, 104413.

Lu, S., Chen, N., Zhou, W. & Li, S. (2024). Impact of the Belt and Road Initiative on trade status and FDI attraction: A local and global network perspective. *International Review of Economics & Finance*, 89, pp.1468–1495.

Martin, T., Zhang, X. & Newman, M.E.J. (2014). Localization and centrality in networks. *Physical Review E*, 90(5), 052808.

Pichler, A., Pangallo, M., del Rio-Chanona, R.M., Lafond, F. & Farmer, J.D. (2022). Forecasting the propagation of pandemic shocks with a dynamic input-output model. *Journal of Economic Dynamics and Control*, 144, 104527.

Ren, Z., Wang, W., Weng, T. & Du, W. (2024). Effects of simplicial centrality on robustness of higher-order multiplex world trade networks. *New Journal of Physics*, 26(11), 113005.

Scheckenhofer, L., Teti, F.A. & Wanner, J. (2025). Dodging trade sanctions? Evidence from military goods. *AEA Papers and Proceedings*, 115, pp.573–577.

Serrano, M.Á. & Boguñá, M. (2003). Topology of the world trade web. *Physical Review E*, 68, 015101.

Segarra, S. & Ribeiro, A. (2016). Stability and continuity of centrality measures in weighted graphs. *IEEE Transactions on Signal Processing*, 64(3), pp.543–555.

Squartini, T., Fagiolo, G. & Garlaschelli, D. (2011). Randomizing world trade. I. A binary network analysis. *Physical Review E*, 84(4), 046117.

Tse, Y.K., Dong, K., Sun, R.Q. & Mason, R. (2024). Recovering from geopolitical risk: An event study of Huawei's semiconductor supply chain. *International Journal of Production Economics*, 275, 109347.

World Bank (2025). *World Integrated Trade Solution (WITS) database*. Washington, DC: World Bank. Available at: https://wits.worldbank.org [Accessed 15 August 2025].

Yan, X. & Piao, L. (2025). The effect of global geopolitical risks on trade openness. *International Review of Economics & Finance*, 102, 104366.

Yassa, A.D. & Yılmaz, K. (2025). Propagation of foreign trade shocks through domestic supply chain networks: Evidence from Turkish firms. Working Paper No. 25/03, Central Bank of the Republic of Türkiye.

Appendix A:

Proof of proposition 1:

Start from the definition of Katz-Bonacich centrality under trade disturbances. Let $\mathbf{1}$ denote the vector of ones and write

$$v^{noisy} = (\boldsymbol{I} - \phi(\boldsymbol{A} + \boldsymbol{N}))^{-1}\mathbf{1} = (\boldsymbol{I} - \phi\boldsymbol{A} - \phi\boldsymbol{N})^{-1}\mathbf{1}.$$

Define

$$\boldsymbol{M} = (\boldsymbol{I} - \phi\boldsymbol{A}),$$

which is invertible under the maintained stability condition, and let

$$\boldsymbol{E} \coloneqq -\phi\boldsymbol{N}.$$

Then

$$v^{noisy} = (\boldsymbol{M} + \boldsymbol{E})^{-1}\mathbf{1}.$$

For small trade disturbances E, the inverse admits a first-order expansion around M,

$$(\boldsymbol{M} + \boldsymbol{E})^{-1} \approx \boldsymbol{M}^{-1} - \boldsymbol{M}^{-1}\boldsymbol{E}\boldsymbol{M}^{-1} + \mathrm{o}\left(\| \underset{\mathbf{E}\to 0}{\boldsymbol{E}} \|\right),$$

where the remainder term vanishes faster than $\| \mathbf{E} \|$ as $\| \mathbf{E} \|$ approaches zero.
Substituting $\boldsymbol{M}^{-\mathbf{1}} = \boldsymbol{G}$ and $\boldsymbol{E} = -\phi\boldsymbol{N}$ yields

$$(\boldsymbol{M} + \boldsymbol{E})^{-1} = \boldsymbol{G} - \boldsymbol{G}(-\phi\boldsymbol{N})\boldsymbol{G} = \boldsymbol{G} + \phi\boldsymbol{GNG}.$$

Applying the expansion to the vector of $\mathbf{1}$

$$\boldsymbol{v}^{noisy} = (\boldsymbol{M} + \boldsymbol{E})^{-1}\mathbf{1} \approx (\boldsymbol{G} + \phi\boldsymbol{GNG})\mathbf{1} = \boldsymbol{G}\mathbf{1} + \phi\boldsymbol{GNG}\mathbf{1}.$$

Recall that baseline Katz Bonacich centrality satisfies

$$\boldsymbol{v} = \boldsymbol{G}\mathbf{1}.$$

Hence, the first-order change in centrality satisfies

$$\Delta\boldsymbol{v} = \boldsymbol{v}^{noisy} - \boldsymbol{v} \approx \phi\boldsymbol{GNG}\mathbf{1} = \phi\boldsymbol{GN}\boldsymbol{v}. \tag{A.1}$$

The expression gives the linear sensitivity of systemic influence to trade disturbances.

To make the dependence on baseline centrality explicit, take norms and apply submultiplicativity of the operator norm $\|\cdot\|$,

$$\|\boldsymbol{ABC}\| \leq \|\boldsymbol{A}\| \|\boldsymbol{B}\| \|\boldsymbol{C}\|$$

which gives:

$$\|\Delta\boldsymbol{v}\| \approx \phi \|\boldsymbol{GN}v\| \leq \phi \|\boldsymbol{G}\| \|\boldsymbol{N}\| \|\boldsymbol{v}\|. \tag{A.2}$$

For fixed ϕ, $\|\boldsymbol{G}\|$, and $\|\boldsymbol{N}\|$, the magnitude of Δv therefore scales proportionally with baseline centrality $\| v \|$. Countries with larger baseline systemic influence thus experience larger adjustments in influence for trade disturbances of a given magnitude.

Appendix B

Table B.1: Calculation of absolute mean volatility (2022) for the United States at $\phi = \frac{90\%}{\lambda\text{max}}$

Noise Level	Influence after noise	Baseline	Absolute difference
10%	19.03	18.94	0.09
20%	19.18	18.94	0.24
30%	19.23	18.94	0.29
40%	20.56	18.94	1.62
50%	19.06	18.94	0.12
60%	21.68	18.94	2.74
70%	22.28	18.94	3.34
80%	19.18	18.94	0.25
90%	18.73	18.94	0.21
Sum			8.90
σ_{v_i}			$\frac{8.90}{9} = 0.99$

Appendix C: Numerical Illustration of the Redistribution Mechanism

To clarify the redistribution rule introduced in Section 3.5, this appendix provides a numerical example based on a six-country trade network. Let country 0 denote the United States, countries 1–3 denote the recipient bloc (France, Germany, and the United Kingdom), and countries 4–5 denote Brazil and India. Let $A = [A_{ij}]$ be the directed export matrix, where A_{ij} denotes exports from country i to country j:

$$A = \begin{bmatrix} 0 & 20 & 15 & 10 & 8 & 7 \\ 12 & 0 & 5 & 4 & 3 & 2 \\ 9 & 6 & 0 & 5 & 2 & 3 \\ 8 & 4 & 3 & 0 & 2 & 2 \\ 7 & 3 & 2 & 2 & 0 & 4 \\ 6 & 2 & 3 & 2 & 5 & 0 \end{bmatrix}$$

For example, $A_{20} = 9$ represents German exports to the United States, while $A_{02} = 15$ represents U.S. exports to Germany.

C.1 Bilateral Export Reduction

Suppose all bilateral export flows involving the United States fall proportionally by 50%. This means that both exports from the United States to its partners and exports from partner countries to the United States are reduced by one half. Formally, for all $j \neq 0$,

$$A_{0j}^{(r)} = (1-\rho)A_{0j}, A_{j0}^{(r)} = (1-\rho)A_{j0},$$

where $\rho = 0.5$. All other bilateral export flows remain unchanged:

$$A_{ij}^{(r)} = A_{ij}, i, j \neq 0.$$

Hence, the reduced matrix is

$$A^{(r)} = \begin{bmatrix} 0 & 10 & 7.5 & 5 & 4 & 3.5 \\ 6 & 0 & 5 & 4 & 3 & 2 \\ 4.5 & 6 & 0 & 5 & 2 & 3 \\ 4 & 4 & 3 & 0 & 2 & 2 \\ 3.5 & 3 & 2 & 2 & 0 & 4 \\ 3 & 2 & 3 & 2 & 5 & 0 \end{bmatrix}$$

This matrix captures the bilateral contraction in export flows involving the United States.

C.2 Decomposition of the Export Loss

The reduction in the first row of Agives the decline in U.S. exports:

$$L^{out} = \sum_{j\in\{1,2,3,4,5\}} (A_{0j} - A_{0j}^{(r)}) = (20 - 10) + (15 - 7.5) + (10 - 5) + (8 - 4) + (7 - 3.5)$$
$$= 30$$

The reduction in the first column gives the decline in exports to the United States:

$$L^{in} = \sum_{i\in\{1,2,3,4,5\}} (A_{i0} - A_{i0}^{(r)}) = (12 - 6) + (9 - 4.5) + (8 - 4) + (7 - 3.5) + (6 - 3) = 21$$

Therefore, the total bilateral export contraction is

$$L^{total} = L^{out} + L^{in} = 30 + 21 = 51$$

C.3 Redistribution Pool

Although bilateral export flows involving the United States fall in both directions, only exports previously destined for the United States are redirected. The economic intuition is that partner countries lose access to the U.S. market and redirect part of those exports toward alternative destinations in the recipient bloc.

Accordingly, the redistribution pool is defined as

$$\mathrm{T}_{\mathrm{lost}} = \mathrm{L}^{\mathrm{in}} = 21$$

The reduction in U.S. exports, L^{out}, reflects lower imports from the United States and is not reallocated under this mechanism.

C.4 Redistribution Weights

Let the recipient set be

$$\varepsilon = \{1,2,3\}$$

Using the reduced matrix $A^{(r)}$, define each recipient country's internal export capacity as

$$\tau_i = \sum_{\substack{j\in\varepsilon \\ j\neq i}} A_{ij}^{(r)}, i \in \varepsilon$$

Thus,

$$\tau_1 = A_{12}^{(r)} + A_{13}^{(r)} = 5 + 4 = 9$$

$$\tau_2 = A_{21}^{(r)} + A_{23}^{(r)} = 6 + 5 = 11$$

$$\tau_3 = A_{31}^{(r)} + A_{32}^{(r)} = 4 + 3 = 7$$

Hence,

$$\sum_{k\in\varepsilon} \tau_k = 9 + 11 + 7 = 27$$

The redistribution weights are therefore

$$w_i = \frac{\tau_i}{\sum_{k\in\varepsilon} \tau_k}$$

so that

$$w_1 = \frac{9}{27}, w_2 = \frac{11}{27}, w_3 = \frac{7}{27}$$

Numerically,

$$w_1 \approx 0.3333, w_2 \approx 0.4074, w_3 \approx 0.2593$$

Appendix D. Alternative Redistribution Schemes

To assess the robustness of the results to the choice of redistribution rule, we consider two alternative allocation schemes in addition to the baseline redistribution proportional to internal export activity within the recipient set ε.

D.1 Equal Redistribution

Under the equal allocation scheme, the total export volume diverted from the United States is distributed uniformly across all recipient countries in ε. Each country $i \in \varepsilon$receives an identical weight:

$$w_i = \frac{1}{|\varepsilon|}$$

Redistributed export flows between any pair $i, j \in \varepsilon$ are defined as:

$$R_{ij}^{\text{equal}} = \frac{1}{|\varepsilon|^2} T_{\text{lost}}$$

This rule abstracts from differences in export size or systemic influence and provides a neutral benchmark in which all recipient countries absorb displaced export flows equally.

D.2 Centrality-Weighted Redistribution

Under the centrality-weighted scheme, displaced export flows are allocated proportionally to countries' baseline systemic importance. Let $v_i$denote the baseline Katz–Bonacich centrality of country $i$in the unshocked network. Redistribution weights are defined as:

$$w_i^{\text{cent}} = \frac{v_i}{\sum_{k \in \varepsilon} v_k}$$

Redistributed export flows between countries $i, j \in \varepsilon$ are then:

$$R_{ij}^{\text{cent}} = w_i^{\text{cent}} w_j^{\text{cent}} T_{\text{lost}}$$

This scheme directs a larger share of displaced export flows toward countries that are already systemically important.

Across both alternative schemes, the qualitative response of aggregate systemic influence to reductions in U.S.-linked export flows remains unchanged. Moderate export reductions initially increase total Katz–Bonacich centrality, while larger reductions reverse this effect. Although the magnitude of the response and the location of the turning point vary slightly across schemes, the overall non-linear pattern persists.

These results indicate that the main findings do not depend on a particular redistribution assumption. Instead, they reflect the underlying structure of global export linkages.

Appendix E

From the model:

$$y = \beta_x x + \beta_d d + \beta_{int}(x \cdot d)$$

The estimated model yields distinct regression lines for centre and periphery countries. For periphery countries ($d = 0$), volatility is given by:

$$y = \beta_x x$$

For centre countries ($d = 1$), volatility is given by:

$$y = (\beta_x + \beta_{int})x + \beta_d$$

This implies both a downward shift in the intercept and a steeper slope for centre countries, consistent with the presence of structural heterogeneity.

Appendix Table E1: Correlation Results (ϕ= 0.9 / λ_{max})

Year	Pearson	Pearson p-value	Spearman	Spearman p-value
2016	0.9824	0.0000	0.1305	0.1116
2017	0.9806	0.0000	0.1565	0.0558
2018	0.9809	0.0000	0.1770	0.0303
2019	0.9760	0.0000	0.1174	0.1525
2020	0.9799	0.0000	0.1461	0.0745
2021	0.9836	0.0000	0.1975	0.0154
2022	0.9758	0.0000	0.1704	0.0371
2023	0.9735	0.0000	0.1298	0.1134

Appendix Table E2: Pooled Regression and Chow Test (ϕ = 0.9 / λ_max)

Year	β_x (Pooled)	R^2 (Pooled)	Chow F	Chow p-value
2016	0.0304	0.9652	84.6443	0.0000
2017	0.0300	0.9616	76.3949	0.0000
2018	0.0298	0.9622	70.3805	0.0000
2019	0.0271	0.9527	73.3131	0.0000
2020	0.0300	0.9603	90.8833	0.0000
2021	0.0344	0.9674	73.1441	0.0000
2022	0.0293	0.9521	70.2026	0.0000
2023	0.0295	0.9476	93.1207	0.0000

Appendix Table E3: Regression Results (ϕ = 0.9 / λ_max)

Year	Threshold	Centre_Count	β_x	β_centre	β_interaction	R² (Dummy)	Adj. R²
2016	4.0986	15	0.0132	-0.0714	0.0211	0.9839	0.9835
2017	4.5913	15	0.0130	-0.0632	0.0205	0.9812	0.9808
2018	4.6781	15	0.0147	-0.0666	0.0189	0.9808	0.9804
2019	5.1699	15	0.0116	-0.0609	0.0190	0.9764	0.9759
2020	5.3308	15	0.0146	-0.0735	0.0196	0.9823	0.9819
2021	5.1556	15	0.0192	-0.0695	0.0192	0.9837	0.9834
2022	5.3491	15	0.0144	-0.0785	0.0194	0.9756	0.9751
2023	5.6593	15	0.0123	-0.0833	0.0222	0.9770	0.9765

Appendix Table E4: Correlation Results (ϕ = 0.5 / λ_max)

Year	Pearson	Pearson p-value	Spearman	Spearman p-value
2016	0.4627	0.0000	-0.6148	0.0000
2017	0.3776	0.0000	-0.5710	0.0000
2018	0.4053	0.0000	-0.6104	0.0000
2019	0.3518	0.0000	-0.6011	0.0000
2020	0.4971	0.0000	-0.5951	0.0000
2021	0.4704	0.0000	-0.5973	0.0000
2022	0.4388	0.0000	-0.5628	0.0000
2023	0.3909	0.0000	-0.6061	0.0000

Appendix Table E5: Pooled Regression and Chow Test (ϕ = 0.5 / λ_max)

Year	β_x (Pooled)	R² (Pooled)	Chow F	Chow p-value
2016	0.0045	0.2140	108.6325	0.0000
2017	0.0035	0.1426	101.7281	0.0000
2018	0.0038	0.1643	81.2182	0.0000
2019	0.0033	0.1238	89.2129	0.0000
2020	0.0051	0.2471	120.5786	0.0000
2021	0.0048	0.2212	103.8693	0.0000
2022	0.0045	0.1925	108.1979	0.0000
2023	0.0041	0.1528	123.9823	0.0000

Appendix Table E6: Dummy Regression Results (ϕ = 0.5 / λ_max)

2016	1.3834	15	-0.0199	-0.0404	0.0310	0.6841	0.6776
2017	1.3884	15	-0.0206	-0.0380	0.0299	0.6418	0.6344
2018	1.3960	15	-0.0182	-0.0353	0.0275	0.6044	0.5963
2019	1.4203	15	-0.0186	-0.0363	0.0278	0.6057	0.5976
2020	1.4485	15	-0.0180	-0.0388	0.0295	0.7161	0.7102
2021	1.4635	15	-0.0178	-0.0375	0.0287	0.6786	0.6720
2022	1.4643	15	-0.0185	-0.0395	0.0296	0.6747	0.6680
2023	1.4705	15	-0.0210	-0.0417	0.0318	0.6860	0.6796

Appendix F

Appendix F_1

QUADRATIC REGRESSION RESULTS: 2016–2023

Year	Phi	Intercept	Linear	Quadratic	r*	R^2	F	Prob(F)
2016	0.5	171.9608	-0.1161	0.000755	76.87	0.9996	115482.45	0.0
2016	0.9	318.4948	-3.3030	0.028597	57.75	0.9596	1164.48	0.0
2017	0.5	172.3171	-0.1163	0.000750	77.53	0.9996	116185.90	0.0
2017	0.9	321.1177	-3.3092	0.028170	58.74	0.9582	1122.40	0.0
2018	0.5	172.8615	-0.1173	0.000766	76.55	0.9996	130711.05	0.0
2018	0.9	328.2185	-3.4687	0.030254	57.33	0.9625	1258.64	0.0
2019	0.5	173.3812	-0.1216	0.000807	75.34	0.9997	142330.52	0.0
2019	0.9	335.2112	-3.7090	0.033442	55.45	0.9655	1371.88	0.0
2020	0.5	172.8567	-0.1146	0.000757	75.65	0.9997	190544.42	0.0
2020	0.9	333.2164	-3.5502	0.031293	56.73	0.9686	1511.38	0.0
2021	0.5	173.2017	-0.1149	0.000750	76.57	0.9997	172369.77	0.0
2021	0.9	334.6594	-3.5123	0.030315	57.93	0.9667	1420.63	0.0
2022	0.5	173.4679	-0.1284	0.000847	75.79	0.9996	125603.30	0.0
2022	0.9	333.0458	-3.7445	0.033063	56.63	0.9608	1199.45	0.0
2023	0.5	173.5663	-0.1302	0.000870	74.80	0.9996	118142.03	0.0
2023	0.9	333.9536	-3.8772	0.035254	54.99	0.9606	1193.40	0.0

PIECEWISE (THRESHOLD) REGRESSION RESULTS: 2016–2023

Year	Phi	r*	Intercept	Initial Slope	Slope Change	Post-r* Slope	R^2	F	Prob(F)
2016	0.5	76.87	171.1468	-0.0550	0.0488	-0.0062	0.9309	659.88	0.0
2016	0.9	57.75	299.9095	-1.5205	1.2717	-0.2488	0.8291	237.68	0.0
2017	0.5	77.53	171.4967	-0.0551	0.0499	-0.0052	0.9311	661.68	0.0
2017	0.9	58.74	302.0134	-1.5152	1.2382	-0.2770	0.8270	234.28	0.0
2018	0.5	76.55	172.0431	-0.0555	0.0490	-0.0065	0.9313	664.76	0.0
2018	0.9	57.33	308.9687	-1.6025	1.3550	-0.2475	0.8338	245.85	0.0
2019	0.5	75.34	172.5442	-0.0575	0.0493	-0.0081	0.9315	666.79	0.0
2019	0.9	55.45	315.6736	-1.7334	1.5305	-0.2029	0.8383	254.03	0.0
2020	0.5	75.65	172.0666	-0.0542	0.0471	-0.0071	0.9325	677.46	0.0
2020	0.9	56.73	313.9493	-1.6504	1.4178	-0.2325	0.8443	265.65	0.0
2021	0.5	76.57	172.4014	-0.0544	0.0484	-0.0061	0.9323	674.94	0.0
2021	0.9	57.93	314.9594	-1.6211	1.3548	-0.2663	0.8411	259.42	0.0
2022	0.5	75.79	172.5790	-0.0607	0.0525	-0.0082	0.9312	662.90	0.0
2022	0.9	56.63	312.5968	-1.7347	1.4893	-0.2454	0.8306	240.31	0.0
2023	0.5	74.80	172.6742	-0.0615	0.0520	-0.0095	0.9308	659.19	0.0
2023	0.9	54.99	313.6620	-1.8120	1.6146	-0.1974	0.8295	238.42	0.0

Appendix F_2

QUADRATIC REGRESSION RESULTS BRICS: 2016-2023

Year	Phi	Intercept	Linear	Quadratic	r*	R²	F	Prob(F)
2016	0.5	171.9192	-0.1334	0.000684	97.61	0.9995	99577.58	0.0
2016	0.9	311.0193	-3.1028	0.021230	73.08	0.9521	973.38	0.0
2017	0.5	172.2787	-0.1327	0.000682	97.22	0.9995	102320.84	0.0
2017	0.9	314.3155	-3.1463	0.021574	72.92	0.9525	981.61	0.0
2018	0.5	172.8203	-0.1341	0.000692	96.87	0.9995	107151.98	0.0
2018	0.9	320.2292	-3.2339	0.022203	72.83	0.9537	1008.52	0.0
2019	0.5	173.3343	-0.1394	0.000725	96.08	0.9995	106120.65	0.0
2019	0.9	325.2155	-3.3434	0.023065	72.48	0.9530	993.79	0.0
2020	0.5	172.8143	-0.1316	0.000677	97.24	0.9996	132029.03	0.0
2020	0.9	324.5170	-3.2670	0.022321	73.18	0.9584	1128.44	0.0
2021	0.5	173.1657	-0.1299	0.000673	96.54	0.9996	133928.65	0.0
2021	0.9	327.4083	-3.2785	0.022527	72.77	0.9587	1137.42	0.0
2022	0.5	173.4208	-0.1482	0.000748	99.02	0.9995	108699.00	0.0
2022	0.9	324.0587	-3.4130	0.023514	72.57	0.9508	946.26	0.0
2023	0.5	173.5125	-0.1509	0.000762	98.98	0.9995	97942.76	0.0
2023	0.9	323.2165	-3.4242	0.023635	72.44	0.9481	894.98	0.0

PIECEWISE (THRESHOLD) REGRESSION RESULTS BRICS: 2016-2023

Year	Phi	r*	Intercept	Initial Slope	Slope Change	Post-r* Slope	R²	F	Prob(F)
2016	0.5	97.61	170.8379	-0.0665	0.5251	0.4586	0.9362	718.56	0.0
2016	0.9	73.08	287.6339	-1.3753	0.8082	-0.5671	0.8327	243.85	0.0
2017	0.5	97.22	171.2046	-0.0660	0.4485	0.3825	0.9359	715.74	0.0
2017	0.9	72.92	290.6590	-1.3947	0.8234	-0.5713	0.8329	244.23	0.0
2018	0.5	96.87	171.7359	-0.0667	0.4057	0.3390	0.9358	714.23	0.0
2018	0.9	72.83	295.9763	-1.4347	0.8531	-0.5817	0.8344	246.93	0.0
2019	0.5	96.08	172.2114	-0.0691	0.3392	0.2701	0.9355	710.43	0.0
2019	0.9	72.48	300.2372	-1.4826	0.8855	-0.5971	0.8330	244.33	0.0
2020	0.5	97.24	171.7497	-0.0655	0.4548	0.3893	0.9362	719.07	0.0
2020	0.9	73.18	300.0495	-1.4545	0.8783	-0.5763	0.8418	260.71	0.0
2021	0.5	96.54	172.1186	-0.0646	0.3649	0.3003	0.9361	717.52	0.0
2021	0.9	72.77	302.9900	-1.4596	0.8884	-0.5712	0.8415	260.20	0.0
2022	0.5	99.02	172.2090	-0.0740	1.1336	1.0596	0.9363	719.75	0.0
2022	0.9	72.57	298.4825	-1.5119	0.8953	-0.6166	0.8303	239.76	0.0
2023	0.5	98.98	172.2786	-0.0754	1.1300	1.0546	0.9362	719.19	0.0
2023	0.9	72.44	297.5235	-1.5141	0.8893	-0.6248	0.8264	233.19	0.0

Appendix F_3

QUADRATIC REGRESSION RESULTS South Peripheral: 2016-2023

Year	Phi	Intercept	Linear	Quadratic	r*	R²	F	Prob(F)
2016	0.5	171.9053	-0.1405	0.000653	107.52	0.9995	101827.27	0.0

2016	0.9	310.1963	-3.1302	0.020818	75.18	0.9537	1009.81	0.0
2017	0.5	172.2650	-0.1400	0.000658	106.40	0.9995	104072.99	0.0
2017	0.9	313.3505	-3.1793	0.021172	75.08	0.9540	1016.35	0.0
2018	0.5	172.8069	-0.1416	0.000672	105.31	0.9995	108428.52	0.0
2018	0.9	319.1362	-3.2722	0.021796	75.06	0.9551	1042.32	0.0
2019	0.5	173.3195	-0.1484	0.000702	105.65	0.9996	110151.08	0.0
2019	0.9	323.9906	-3.3851	0.022581	74.95	0.9547	1031.62	0.0
2020	0.5	172.8011	-0.1403	0.000654	107.17	0.9996	135668.72	0.0
2020	0.9	323.3922	-3.3087	0.021888	75.58	0.9597	1165.95	0.0
2021	0.5	173.1518	-0.1391	0.000654	106.29	0.9996	136641.40	0.0
2021	0.9	326.0321	-3.3281	0.022041	75.50	0.9600	1175.37	0.0
2022	0.5	173.4080	-0.1524	0.000744	102.44	0.9995	99491.42	0.0
2022	0.9	322.9462	-3.4326	0.023119	74.24	0.9510	951.10	0.0
2023	0.5	173.5028	-0.1551	0.000767	101.09	0.9995	93199.81	0.0
2023	0.9	322.2066	-3.4491	0.023361	73.82	0.9485	902.72	0.0

PIECEWISE (THRESHOLD) REGRESSION RESULTS South Peripheral: 2016–2023

Year	Phi	r*	Intercept	Initial Slope	Slope Change	Post-r* Slope	R^2	F	Prob(F)
2016	0.5	100.00	170.8274	-0.0751	0.0000	-0.0751	0.9507	1908.31	0.0
2016	0.9	75.18	286.0920	-1.3923	0.7982	-0.5941	0.8392	255.63	0.0
2017	0.5	100.00	171.1796	-0.0742	0.0000	-0.0742	0.9488	1836.08	0.0
2017	0.9	75.08	288.8979	-1.4141	0.8127	-0.6014	0.8393	255.93	0.0
2018	0.5	100.00	171.6974	-0.0744	0.0000	-0.0744	0.9469	1766.70	0.0
2018	0.9	75.06	294.0043	-1.4564	0.8421	-0.6144	0.8407	258.68	0.0
2019	0.5	100.00	172.1608	-0.0782	0.0000	-0.0782	0.9475	1788.47	0.0
2019	0.9	74.95	298.0118	-1.5061	0.8705	-0.6356	0.8400	257.21	0.0
2020	0.5	100.00	171.7214	-0.0748	0.0000	-0.0748	0.9502	1890.05	0.0
2020	0.9	75.58	297.9898	-1.4788	0.8737	-0.6051	0.8481	273.57	0.0
2021	0.5	100.00	172.0723	-0.0737	0.0000	-0.0737	0.9488	1833.13	0.0
2021	0.9	75.50	300.5133	-1.4876	0.8814	-0.6063	0.8484	274.17	0.0
2022	0.5	100.00	172.1808	-0.0780	0.0000	-0.0780	0.9413	1588.69	0.0
2022	0.9	74.24	296.7089	-1.5225	0.8743	-0.6483	0.8337	245.67	0.0
2023	0.5	100.00	172.2370	-0.0784	0.0000	-0.0784	0.9384	1507.26	0.0
2023	0.9	73.82	295.8979	-1.5269	0.8734	-0.6535	0.8296	238.57	0.0

Appendix G:

Section 4. Proof hypothesis 5a

The Katz-Bonacich centrality:

$$v = \left(\boldsymbol{I} - \phi\widetilde{\boldsymbol{A}}(r)\right)^{-1}\mathbf{1},\ \widetilde{\boldsymbol{A}}(r) = \boldsymbol{A} + \boldsymbol{R}(r) \tag{G1}$$

Expand using Neumann series:

$$\left(\boldsymbol{I} - \phi\widetilde{\boldsymbol{A}}(r)\right)^{-1} = I + \phi\widetilde{\boldsymbol{A}}(r) + \ \phi^2\widetilde{\boldsymbol{A}}(r)^2 + \phi^3\widetilde{\boldsymbol{A}}(r)^3 + \cdots \tag{G2}$$

Then, decompose powers of $\widetilde{\boldsymbol{A}}(r)$

$\widetilde{\boldsymbol{A}}(r)^2 = \left(\boldsymbol{A} + \boldsymbol{R}(r)\right)^2 = \boldsymbol{A}^2 + \boldsymbol{A}\boldsymbol{R}(r) + \boldsymbol{R}(r)\boldsymbol{A} + \boldsymbol{R}(r)^2$ (G3)

$$\widetilde{\boldsymbol{A}}(r)^3 = \left(\boldsymbol{A} + \boldsymbol{R}(r)\right)^3 = \boldsymbol{A}^3 + \cdots + \boldsymbol{R}(r)^3 \tag{G4}$$

Higher terms in $\boldsymbol{R}(r)$: $\boldsymbol{A}\boldsymbol{R}(r) + \boldsymbol{R}(r)\boldsymbol{A}$ (G5)

Higher-order terms: $\boldsymbol{R}(r)^2$, $\boldsymbol{R}(r)^3$, etc.

For small redistributions, higher-order terms are negligible, so we can truncate at first order.

$$\Delta v_i(r) = \underbrace{\phi \textstyle\sum_j \boldsymbol{R_{ij}}(r) +}_{\text{the direct effect}} \underbrace{\phi^2 \textstyle\sum_{j,k} \boldsymbol{R_{ij}}(r)\boldsymbol{A_{ik}} + \phi^3 \textstyle\sum_{j,k,l} \boldsymbol{R_{ij}}(r)\boldsymbol{A_{jk}}\boldsymbol{A_{kl}} + \dots}_{\text{indirect effects}}.$$

The first-order term $\phi \sum_j \boldsymbol{R}(r)\,[i,j]$ gives immediate gains for nodes that receive redistributed trade directly, typically already central nodes.

Higher-order terms $(\phi^2, \phi^3, \dots)$ explain delayed gains for peripheral nodes, as redistribution propagates through multi-step paths in the baseline network $\boldsymbol{A}$.

This expansion clarifies why central nodes benefit immediately from redistribution, while weaker nodes accumulate influence only as shocks deepen and multi-step network effects accumulate.

Appendix H. Generalised Trade Reallocation Framework

The baseline simulations in the main text consider a four-country recipient bloc under a specific redistribution rule. This appendix develops a more general formulation that allows the number of recipient countries, the degree of successful reallocation, and the extent of aggregate contraction to vary explicitly.

Consider the baseline export matrix $\boldsymbol{A} = [\boldsymbol{A}_{ij}]$, where $\boldsymbol{A}_{ij}$ denotes exports from country i to country j. The United States is indexed by u, while i and j refer to any countries other than the United States acting as exporter and importer, respectively. The parameter $r \in [0,1]$ denotes the proportional reduction in bilateral export flows involving the United States, so that $r = 0.30$ corresponds to a 30 percent shock.

For any shock size r, define the reduced matrix $\boldsymbol{A}^{(r)}$ by

$$\boldsymbol{A}_{uj}^{(r)} = (1-r)\boldsymbol{A}_{uj}, \boldsymbol{A}_{iu}^{(r)} = (1-r)\boldsymbol{A}_{iu}, \text{for } i, j \neq u \tag{H.1}$$

with all remaining entries unchanged.

These expressions imply that the initial shock proportionally reduces all export flows connected to the United States. The first term refers to U.S. exports to partner countries, while the second refers to partner-country exports to the United States. Hence, if $r = 0.30$, every export link involving the United States falls by 30 percent, whereas export links between all other countries remain unchanged at this stage.

Let $\mathcal{E}_m$ denote a recipient bloc containing m countries, where m is not restricted to four. The loss of exports previously destined for the United States is given by

$$L^{in}(r) = \sum_{i \neq u} \left(\boldsymbol{A}_{iu} - \boldsymbol{A}_{iu}^{(r)} \right) \tag{H.2}$$

and the reduction in U.S. exports to the rest of the world is

$$L^{out}(r) = \sum_{j \neq u} \left(\boldsymbol{A}_{uj} - \boldsymbol{A}_{uj}^{(r)} \right). \tag{H.3}$$

To allow for incomplete diversion, let $\eta \in [0,1]$ denote the share of displaced exports that can be successfully redirected. The effective redistribution pool is therefore

$$T_m(r) = \eta L^{in}(r). \tag{H.4}$$

For each recipient country $i \in \mathcal{E}_m$, define absorptive capacity as

$$\tau_i^{(m)}(r) = \sum\nolimits_{\substack{j \in \mathcal{E}_m \\ j \neq i}} \boldsymbol{A}_{ij}^{(r)}. \tag{H5}$$

The associated redistribution weights are

$$w_i^{(m)}(r) = \frac{\tau_i^{(m)}(r)}{\sum_{k \in \mathcal{E}_m} \tau_k^{(m)}(r)}. \tag{H.6}$$

where τ_i country i's existing export connections within the recipient bloc.

The redistribution matrix is then

$$\boldsymbol{R}_{ij}^{(m,\eta)}(r) = \begin{cases} w_i^{(m)}(r)\, w_j^{(m)}(r)\, T_m(r), & i, j \in \mathcal{E}_m,\ i \neq j \\ 0, & \text{otherwise.} \end{cases} \tag{H.7}$$

The final adjusted network becomes

$$\widetilde{\boldsymbol{A}}^{(m,\eta)}(r) = \boldsymbol{A}^{(r)} + \boldsymbol{R}^{(m,\eta)}(r). \tag{H.8}$$

Systemic influence is evaluated using Katz–Bonacich centrality:

$$v^{(m,\eta)}(r) = \left(I - \phi \widetilde{\boldsymbol{A}}^{(m,\eta)}(r)\right)^{-1} \mathbf{1}, \tag{H.9}$$

with aggregate centrality

$$\mathcal{C}^{(m,\eta)}(r) = \mathbf{1}^\top v^{(m,\eta)}(r). \tag{H.10}$$

The baseline simulations in the paper correspond to the restricted case $m = 4$with full redirection of exports previously destined for the United States under the chosen weighting rule. The broader formulation clarifies that larger recipient sets increase potential absorptive capacity, while higher reallocation efficiency reduces the aggregate losses associated with the initial shock. Under sufficiently broad recipient sets and low adjustment frictions, the decline in aggregate centrality may be substantially weaker than in the benchmark simulations.

Appendix I. Trade Reallocation as a Network Design Problem

The framework can also be interpreted as a policy design problem. Instead of treating trade shocks only as disruptive events, one may ask how displaced exports should be reassigned to maximise aggregate network connectivity after the initial shock. Let $A^{(r)}$denote the reduced export matrix generated by a shock of size r, and let G represent a candidate recipient bloc or, more generally, any admissible redistribution rule. The adjusted network is

$$\widetilde{\boldsymbol{A}}(r, G) = \boldsymbol{A}^{(r)} + \boldsymbol{R}(r, \boldsymbol{G}), \tag{I.1}$$

where $R(r, G)$is the redistribution matrix implied by the chosen allocation rule.

Systemic influence is again measured by Katz–Bonacich centrality:

$$v(r, \boldsymbol{G}) = \left(I - \phi \widetilde{\boldsymbol{A}}(r, \boldsymbol{G})\right)^{-1} \mathbf{1}, \tag{I.2}$$

with aggregate connectivity defined as

$$\mathcal{C}(r, \boldsymbol{G}) = \mathbf{1}^{\top} v(r, \boldsymbol{G}) = \sum_{i=1}^{n} v_i\,(r, \boldsymbol{G}). \tag{I.3}$$

The planner's problem is to choose the shock configuration and redistribution structure that maximises aggregate connectivity:

$$\max_{r,G}\ \mathcal{C}(r, \boldsymbol{G}) \text{ s. t } 0 \leq r \leq 1, \boldsymbol{R}_{ij}(r, \boldsymbol{G}) \geq 0, \sum\nolimits_{i,j} R_{ij}\,(r, \boldsymbol{G}) = T_{lost}(r), \tag{I.4}$$

where $T_{lost}(r)$denotes the volume of exports available for reallocation after the initial reduction in U.S.-related flows.

Two objects of interest follow immediately. The first is the turning point r^*, which identifies the shock magnitude at which aggregate losses are greatest or begin to moderate. The second is the optimal redistribution rule $\boldsymbol{G}^*$, which identifies the allocation structure that yields the highest attainable level of systemic connectivity after the shock.

When the recipient bloc is fixed ex ante, the problem reduces to a one-dimensional choice over the shock parameter:

$$\max_{r} \ \mathcal{C}(r). \tag{I.5}$$

If aggregate centrality is approximated by the quadratic specification estimated in the main text,

$$\mathcal{C}(r) = \alpha + \beta r + \gamma r^2, \tag{I.6}$$

the turning point is

$$r^* = -\frac{\beta}{2\gamma}. \tag{I.7}$$

This provides a tractable empirical rule for identifying the level of trade reallocation at which losses stop intensifying and network adjustment effects become stronger.

More broadly, this optimisation perspective extends the interpretation of the model. The relevant policy question is not only how disruptions reduce connectivity, but also how displaced exports may be redirected to preserve resilience within the international system.